UNIVERSITY OF CALIFORNIA, SAN DIEGO

Strategies for Developing a Benchtop Biosensor for the Rapid Detection of L-Alanine

A thesis submitted in partial satisfaction of the requirements for the degree of Master of Science

in

Bioengineering

by

Jason Anthony Gabunilas

Committee in charge:

David A. Gough, Chair
Dale A. Baker
John T. Watson
Immo E. Scheffler

2011

The Thesis of Jason Anthony Gabunilas is approved and it is acceptable in quality and form for publication on microfilm and electronically:

_____

_____

_____

_____

Chair

University of California, San Diego

2011

TABLE OF CONTENTS

NOMENCLATURE

AlaDH	alanine dehydrogenase
ALAT	alanine aminotransferase
ALT	alanine transaminase
GluOD	glutamate oxidase
GPT	glutamic-pyruvic transaminase
K_m	Michaelis-Menten constant
LDH	lactate dehydrogenase
mL	milliliter
mM	millimolar
mV	millivolt
nA	nanoampere
Pt	platinum
PTFE	polytetrafluoroethylene
PyOD	pyruvate oxidase
SHL	salicylate hydroxylase
V	volt
µL	microliter

LIST OF FIGURES

LIST OF TABLES

ACKNOWLEDGEMENTS

I would like to thank Professors Gough, Watson, and Scheffler for their willingness to assist me with the preparation of this thesis. I am eternally grateful to my advisor Dr. Dale Baker for his mentorship and guidance over the past three years, which has not only culminated in a successful project, but has also driven my development as a scientist and engineer. I would like to extend my gratitude to Lorenzo D'Amico, Justin Yeap, Si Luo, and Andrew Basilio, whose previous work laid the essential foundations for this project. Finally, my heartfelt thanks go to Christopher Peterson for his much-appreciated help with the 3D illustrations in this thesis.

ABSTRACT OF THE THESIS

Strategies for Developing a Benchtop Biosensor for the Rapid Detection of L-Alanine

by

Jason Anthony Gabunilas

Master of Science in Bioengineering

University of California, San Diego, 2011

David A. Gough, Chair

As the subtle intricacies of mammalian metabolism have become further elucidated over the past several decades, substantial progress has been made in the medical and scientific communities to address metabolic disorders and the relationships between abnormalities in metabolism at the molecular level and their observable physiological ramifications. The amino acid alanine is known as a key molecule in protein and carbohydrate metabolism and nitrogen regulation, and has further been associated with a number of diseases and pathological conditions. It is also of interest to the commercial and biotechnological industries. Therefore, a rapid and inexpensive procedure for the measurement of alanine in biological or commercial samples would be of great use.

Two amperometric methods for the measurement of L-alanine involving enzymatic biosensors are explored. The electrochemical foundations for the operation of the sensors are described. The unique reaction mechanism for the conversion of alanine to measurable products is discussed. Sensors are tested for alanine measurement via the oxidation of hydrogen peroxide and the reduction of oxygen. The response of the sensors to reacted alanine samples as well as standard solutions are evaluated with regards to sensitivity and rapidity. These studies show that

the proposed reaction mechanism for alanine conversion and detection is feasible and that the development of an amperometric biosensor for this purpose is an attainable goal, while also suggesting that optimizing the sensitivity of the sensors is paramount to its utility.

CHAPTER 1

INTRODUCTION

L-alanine is a non-essential amino acid that has largely gone unexplored within the realm of discrete or continuous metabolic monitoring. Indeed, as many metabolic disorders such as diabetes are characterized by abnormal blood concentrations of glucose, pyruvate, and other small molecule metabolites, much less attention has been granted to alanine and other higher-order molecules that are not thought to represent a significant link to disease or illness.

The physiological functions of alanine are well-documented and understood. Structurally, it is a simple non-polar amino acid that serves as a building-block for a countless number of proteins, and comprises about 5-7% of protein in muscles [1]. Alanine also serves several important metabolic roles. Ammonia is a toxic compound that accumulates in the bloodstream as a result of normal amino acid catabolism [2], which in turn results in the collection of amino groups in the form of glutamate in tissues. A transamination reaction between glutamate and pyruvate (the latter being the final product of anaerobic metabolism) is then catalyzed by the enzyme alanine aminotransferase (ALAT), also known as glutamic pyruvic transaminase (GPT) and alanine transaminase (ALT), forming L-alanine and α-ketoglutarate. Alanine therefore serves as the principal transport molecule for ammonia, carrying it through the bloodstream to the liver for eventual excretion in urine via the urea cycle, and in so doing providing a means by which muscles can eliminate excess nitrogen. The reverse of the ALAT reaction can also be utilized to produce pyruvate as a fuel for gluconeogenesis [3].

1.1. Motivation for Alanine Measurement

Researchers have become increasingly interested in monitoring alanine in clinical, commercial, and biotechnological settings. Several investigations have identified blood alanine concentrations with certain physiological conditions: low plasma alanine concentrations have been associated with ketotic hypoglycemia, in which a large increase in the levels of ketones in the body occurs simultaneously with low blood glucose levels [4]. More recently, a 2008 study on human metabolic phenotypes spanning four countries and several thousand test subjects concluded that a strong association exists between high alanine levels brought about by diets rich in alanine-concentrated meat products and high blood pressure [5], a major indication of cardiovascular health. Alanine measurement has also become a topic of interest for researchers in sports medicine due to the role of alanine as a primary substrate for gluconeogenesis. During periods of highly intense anaerobic exercise in which glucose is very rapidly consumed by muscle cells, blood alanine concentrations increase as the body attempts to supply the liver with additional alanine. The liver utilizes alanine to produce pyruvate through transamination, which is then converted to glucose via gluconeogenesis. Furthermore, alanine concentrations tend to remain high relative to other amino acids during periods of exhaustive endurance exercise, and it has been suggested that alanine is synthesized *de novo* in muscle tissue under such conditions [1, 6]. While lactate remains the predominant substrate of interest in most sports medicine laboratory tests, alanine assays may reveal interesting insights on carbohydrate metabolism related to exercse. Finally, gluconeogenesis is also intricately linked with fasting and extreme starvation, and so implications of gluconeogenesis derived from alanine assays could potentially be applied to the study of these conditions, as well.

Outside of medicine, alanine assays are utilized in the food industry to evaluate the nutritional value of various foodstuffs [7]. Additionally, it is a metabolite of interest in the production of certain alcoholic beverages, where L- to D-alanine ratios have important implications in the process of fermentation [8].

Various guides also report the importance of alanine monitoring in cell culture and bioreactor culture processes, which are becoming increasingly common in biotechnology. In bioreactor cell culture, alanine may accumulate as a result of a shift in metabolic machinery in which glutamine replaces glucose as the principal source of energy, accompanied by a decrease in oxygen consumption. Subsequent glutamine depletion is followed by alanine consumption in order to generate pyruvate for gluconeogenesis, an indication of imminent cell death [9]. High alanine concentrations in fed-batch bioreactor cultures may also be indicative of overflow metabolism of glucose, resulting in the accumulation of lactate and encouraging overly-acidic conditions [10]. Abnormally high bioreactor culture alanine concentrations may also indicate excessive ammonia production, with excess ammonia transferred from glutamate to pyruvate to form alanine. Ammonia is very toxic to animal cells at high concentrations, and so the monitoring of alanine for purposes of proper nitrogen metabolism may also be of interest.

1.2. Current Alanine Assay and Detection Techniques

Several laboratory techniques exist for the measurement of alanine concentrations in a sample. Although they vary in methodology, most measurement strategies employ active enzymes in order to generate a product from alanine that can be readily measured by a variety of methods. Typical L-alanine assay kits rely on the conversion of L-alanine to pyruvate, which is then detected with colorimetry or fluorescence spectroscopy. Alternatively, the pyruvate participates in a second reaction, such as a reduction reaction with NADH, and the disappearance of NADH resulting from the reaction is measured fluorometrically. These measurements are then compared to a set of alanine standards in order to calculate alanine concentration in the sample [11]. Although time-consuming, these methods are currently the most commonly employed means for measuring alanine. There are also alanine detection methods that rely on high

performance liquid chromatography, which have been successfully integrated into cell culture bioreactor processes [12].

More recently, investigators have ventured into the construction of benchtop *in vitro* alanine biosensors. The basic operation of such sensors remains firmly grounded in the enzymatic conversion of alanine to desirable products via the utilization of various enzymes. However, in each of these approaches the detection ultimately culminates in a redox reaction at an electrode, resulting in the generation of a measurable electric current. The essential elements of enzyme electrodes are discussed next.

1.3. The Principles of Enzymatic Biosensor Operation

Most enzyme electrodes are based on the concept of driving a redox reaction at a working electrode in order to generate a measurable current or potential difference. One or more diffusion-controlled enzymatic reaction steps preceding the final redox reaction ensures that the amplitude of the measurement is proportional to the concentration of the substrate of interest. Figure 1.1 presents a highly schematic depiction of basic electrode design. The primary player in the ensemble is the immobilized enzyme layer, which typically consists of one or more enzymes covalently attached to a membrane material through crosslinking. The enzyme(s) used are specific to the substrates being measured. The immobilized enzyme layer is overlaid by a dialysis membrane layer that limits the diffusion of substrate to the enzyme layer, thereby preventing the reaction from becoming enzyme-limited. A third layer is placed below the enzyme layer that serves as another barrier permitting only certain small molecules. namely the redox substrate, to pass through. This triple-layer arrangement is positioned over a working electrode to create the functional sensor. In some designs, metabolic products generated by the enzymatic reactions diffuse to the electrode where the subsequent redox reaction induces an electron flow as a measurable current. In others, the redox substrate is already present in the bulk solution and is

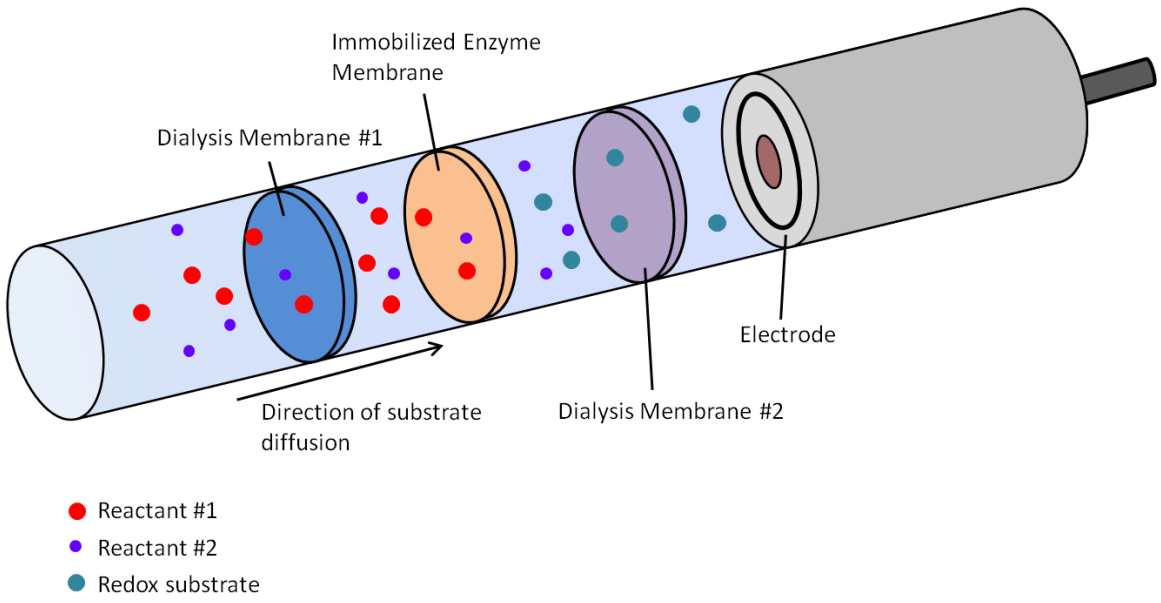

Figure 1.1. Schematic diagram of immobilized enzyme electrode design. The layers of the membrane are shown separated here for the purpose of explanation. In the actual membrane, the layers are very closely stacked together.

consumed along with the analyte of interest in a specific reaction, with the subsequent drop in current due to the consumption of the electrolyzed substance being proportional to the concentration of the analyte. Still other designs do not utilize enzyme immobilization at all and instead rely on the chemical reactions in a freely suspended medium.

Regardless of the substrate measured, benchtop biosensors must meet particular basic requirements. First, it must be able to accurately measure concentrations of substrate within the ranges that are expected during its planned application without relying on extrapolation. These ranges may vary considerably between physiological conditions and batch operation processes, and the sensor apparatus must be designed to suit the conditions. Second, the sensor must have an acceptable response time so that measurements can be obtained in a timely manner. Third, it must give accurate and reliable measurements for the duration of its operational life. Finally, it must be highly specific to the substrate of interest so that other electrochemically-active compounds will not interfere with the measurement.

1.4. Amperiometric Alanine Sensors Developed by Other Investigators

Recent interest in alanine detection has motivated several investigators to explore means of measuring alanine concentrations amperometrically, primarily due to its convenience and reduced assay time when compared to traditional fluorometric or colorimetric methods. Three such endeavors are briefly summarized here.

An early investigation into development of alanine biosensors did not make use of enzyme immobilization [7]. Rather, the measureable substrate was generated by a series of two reactions in free solution in a reaction chamber. The first reaction, catalyzed by alanine dehydrogenase (AlaDH), generates pyruvate and NADH as its primary products:

$$Alanine + NAD^+ + H_2O \rightleftharpoons Pyruvate + NADH + NH_3 + H^+ \quad (1)$$

Whereas traditional assays rely on measuring the absorbance of NADH, the investigators instead implemented a second enzyme, diaphorase, which consumes NADH in the conversion of hexacyanoferrate(III) to hexacyanoferrate(II):

$$2Fe(CN)_6^{3-} + NADH \rightleftharpoons 2Fe(CN)_6^{4-} + NAD^+ + H^+ \quad (2)$$

Hexacyanoferrate(II) would subsequently diffuse through a semi-permeable membrane to the platinum electrode, where the final oxidation reaction generated a current.

$$2Fe(CN)_6^{4-} \rightleftharpoons 2Fe(CN)_6^{3-} + e \quad (3)$$

The steady-state current was proportional to the concentration of hexacyanoferrate(II) and therefore also proportional to the concentrations of NADH and L-alanine. Testing blood and fermentation media samples of varying substrate concentrations, the investigators reported average steady-state current achievement times of less than 10 minutes per sample, strong agreement with concurrent spectrophotometric measurements, and a sensor lifetime over one month with proper handling.

The enzyme immobilization approach was explored by another group of investigators who immobilized three enzymes within a poly(carbamoyl) sulfonate hydrogel upon a polytetrafluoroethylene (PTFE, aka Teflon) membrane [13]. The enzymes employed in the immobilized membrane were alanine dehydrogenase, pyruvate oxidase (PyOD), and salicylate hydroxylase (SHL), where AlaDH catalyzed reaction (1) as shown above and the two other enzymes catalyzed the following reactions:

PyOD: $Pyruvate + Phosphate + O_2 \rightleftharpoons Acetylphosphate + H_2O_2 + CO_2$ (4)

SHL: $Salicylate + NADH + O_2 \rightleftharpoons Catechol + NAD^+ + CO_2$ (5)

By consuming pyruvate and NADH produced by reaction (1), the reaction equilibrium was maintained on the product side. Both reactions resulted in the proportional consumption of dissolved oxygen, which diffused to the silver electrode and was consumed in the reduction reaction. The decrease in amplitude of the oxygen-mediated current following the three-step reaction provided a quantitative measure of the amount of oxygen consumed, and thus the concentration of alanine. Steady-state oxygen currents were achieved following roughly 150s of incubation time.

Previous work conducted by a group of UC San Diego undergraduate students in 2009 explored a strategy combining enzyme immobilization with reaction in solution [14]. The design consisted of a Clark oxygen electrode situated below a reaction chamber that amperometrically measured the oxygen concentration of the liquid sample in the chamber. The group pursued a two-enzyme system consisting of alanine dehydrogenase in free solution and pyruvate oxidase immobilized in an albumin membrane with the use of a glutaraldehyde crosslinker. The membrane was positioned above the oxygen-sensing electrode. Upon the addition of a sample, reaction (1) catalyzed by AlaDH would result in the production of pyruvate, which is then consumed along with oxygen in reaction (2) by the immobilized PyOD. Oxygen reduction at the electrode produced a current proportional the chamber oxygen concentration, with changes in amplitude being proportional to the amount of oxygen consumed and the concentration of substrate. Unfortunately, the sensor in its entirety did not function due to the absence of the cofactor NAD^+ in the solution, thereby preventing reaction (1) from occurring, in addition to the reaction requiring pH ranges that were not easily obtained. However, direct pyruvate injections

did produce current drops (measured as voltage decrease) within 2 minutes, testifying to the soundness of the PyOD immobilization procedure.

1.5. Thesis Organization

This thesis provides a summary of preliminary research towards a novel approach for the rapid *in vitro* measurement of L-alanine using a benchtop enzymatic biosensor, in which two different strageties are explored. The first relies on the implementation of a two-enzyme scheme consisting of two physically separate two chemical reactions and culminates in the oxidation of hydrogen peroxide (H_2O_2) for the detection of L-alanine. The details of the experimental setup and results of this approach are outlined in Chapter II. An alternative approach is also explored that utilizes the same two-enzyme system, but relies instead on the reduction of oxygen to generate a measurable current. The motivations for this design as well as results will be elucidated in Chapter III. A summary of the thesis and possible directions for future research endeavors on this topic is given in Chapter IV.

Chapter II

Alanine Measurements via the Detection of Hydrogen Peroxide

2.1. Introduction

Most amperometric biosensor assay strategies for the detection of L-alanine have involved the use of at least one of alanine dehydrogenase (AlaDH) and pyruvate oxidase (PyOD). Although alanine aminotransferase (ALAT) assays do exist as a means for measuring the concentration of this enzyme in serum or plasma samples, strategies that employ this enzyme for the measurement of alanine concentrations in a given sample have enjoyed very little exploration. In one of the few studies addressing the use ALAT specifically for this purpose, Karl et al. incorporated ALAT into a two-step reaction process that first converts alanine to pyruvate. Next, the resulting pyruvate was converted to lactate by the enzyme lactate dehydrogenase (LDH), a reaction that required the reduction power of NADH. As NADH was consumed, its disappearance was measured fluorometrically [15]. While it was reported to be an accurate method that could used to conduct multiple assays at once, it suffers from the time-consuming preparation steps that tend to plague fluorometric detection schemes and is more suitable for measurements involving tissue samples in which preparation times are already extensive. At the time of this writing, alanine measurement methodologies that make use of ALAT in tandem with amperometric detection techniques are virtually nonexistent. The reasons for the lack of investigation in applying the enzyme in this manner are not fully understood and perhaps may be elucidated in this present investigation.

The overall approach involves a two-reaction mechanism. In the first reaction, ALAT catalyzes the transamination reaction between L-alanine and α-ketoglutarate to form pyruvate and L-glutamate:

$$\text{ALAT: } L-alanine+\alpha-ketoglutarate \rightleftharpoons Pyruvate+L-glutamate \quad (6)$$

The second reaction involves the oxidation of L-glutamate by glutamate oxidase (GluOD), resulting in the reconstitution of α-ketoglutarate and the production of hydrogen peroxide (H_2O_2):

$$\text{GluOD: } L-glutamate+O_2+H_2O \rightleftharpoons \alpha-ketoglutarate+NH_3+H_2O_2 \quad (7)$$

The reactions are physically isolated, with (6) taking place in a standard 1 cm spectrophotometry cuvette. Discrete samples from this reaction are then transferred to a YSI Immobilized Enzyme Biosensor, where reaction (7) occurs. Hydrogen peroxide generated from (7) is then amperometrically measured at the platinum electrode:

$$\text{Pt Electrode: } H_2O_2 \rightarrow 2H^+ + O_2 + 2e^- \quad (8)$$

The resulting current is reported in nanoamperes (nA) by the YSI device.

Figure 2.1 is an adaptation of Figure 1.1 that highlights the different layers of the sensor apparatus involved in (7) and (8). The sensor is covered with a YSI-manufactured glutamate oxidase membrane that is exposed to the solution in the reaction chamber. The top layer is a polycarbonate layer that limits substrate diffusion, followed by an enzyme layer consisting of immobilized glutamate oxidase that catalyzes reaction (7), and ending with a cellulose acetate layer that allows only small molecules such as hydrogen peroxide to diffuse to the electrode.

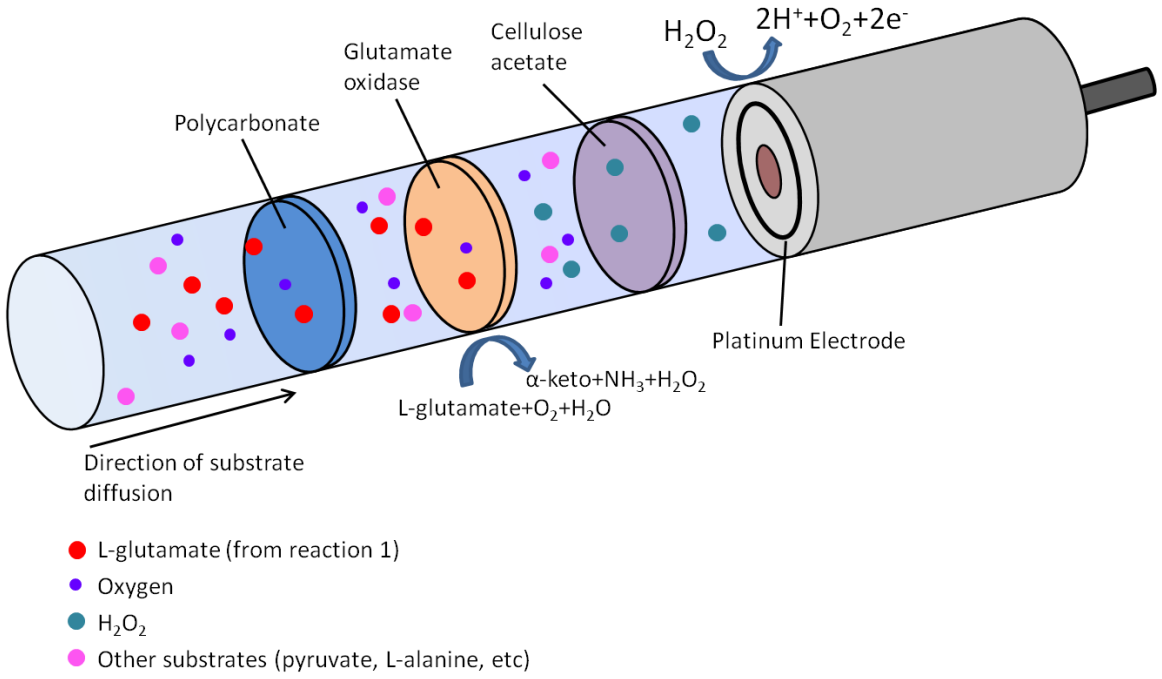

Figure 2.1. Schematic illustration of YSI glutamate oxidase electrode assembly. The generalized membranes have been specified and the chemical reactions have been included.

2.2. Setup of Experimental Equipment and Methods

2.2.1. Glutamate Sensor Calibration

Calibration of the YSI 1500 enzyme sensor was required prior to each assay. Figure 2.2 provides a schematic illustration of the YSI sensor apparatus with frontal and top-down perspectives. All reactions involving glutamate occurred in a 500 μL reaction chamber containing YSI 2357 sensor buffer kept under constant agitation with a stir bar. The buffer was composed of 6.35 g of concentrate dissolved in 450 mL of deionized water, with the concentrate containing disodium phosphate, monosodium phosphate, sodium benzoate, dipotassium EDTA, sodium chloride, and gentamicin sulfate [16]. The sensor was calibrated with buffer solution representing 0 mM glutamate as well as 5 mM and 10 mM glutamate standard solutions purchased from YSI. Standards were introduced via 25 μL syringe-pette injections into the reaction chamber. Upon injection, the sensor was allowed to stabilize its for one minute according the manufacturer's protocol, and the resulting amperage was recorded. Then fresh buffer was cycled into the chamber with a pump mechanism, with the resulting stable current representing the 0 mM glutamate current. In this manner, each calibration consisted of three current measurements each at 5 mM and 10 mM glutamate, and six measurements at 0 mM glutamate, with the estimated "true" value taken as the average for each set. The concentration of α-ketoglutarate utilized in this experiment was 10 mM, ensuring that the glutamate produced in the ALAT reaction would be less than or equal to that concentration (see section 2.2.2 below). Therefore, all measurements for glutamate fell within the range of the calibration (0 to 10 mM), and no extrapolation of the calibration curve was necessary for the calculation of glutamate concentrations during the actual assays.

The average measured currents were then plotted against their corresponding glutamate standard concentrations to construct a calibration curve. Current was chosen as the independent variable because subsequent alanine assays would require the calculation of glutamate/alanine

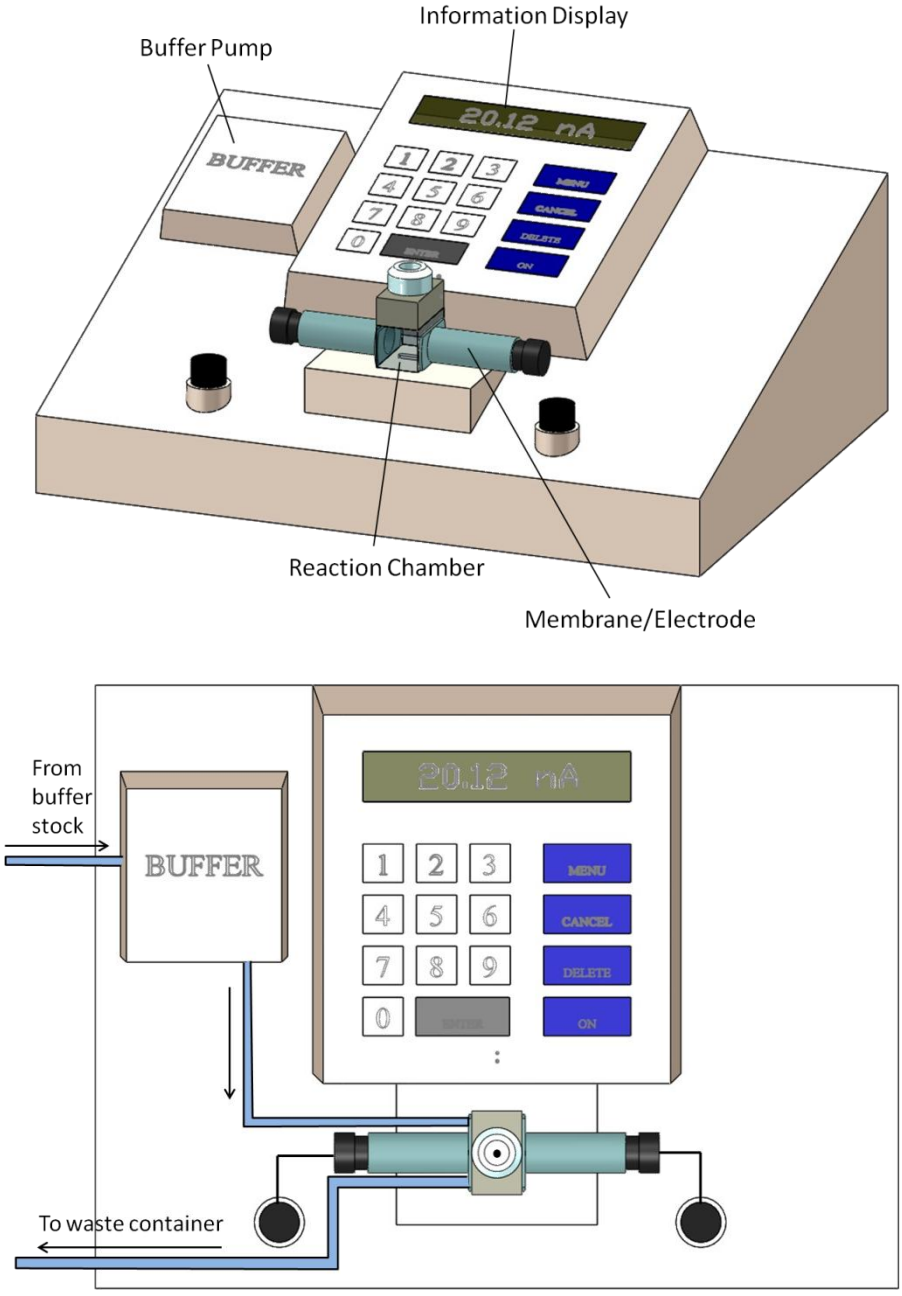

Figure 2.2. Frontal and top-down perspective views of YSI glutamate sensor apparatus

concentration from the measured current. The equation for the line of best fit therefore provided a means for calculating unknown glutamate concentrations in the sample by substituting the current measurements, with the slope corresponding to the sensitivity of the device in millimolar per nanoampere (mM/nA). The calibrations revealed a strong linear relationship between glutamate concentrations and measured current.

2.2.2 Alanine Aminotransferase Reaction

The alanine aminotransferase reaction was prepared and conducted in a 1 cm spectrophotometry cuvette and was modified from a portion of a GPT enzymatic assay protocol prepared by Sigma-Aldrich [17]. A 29 mL reaction cocktail was prepared containing the following components:

1. 20 mL of 100 mM Tris buffer, prepared by dissolving solid Tris base in deionized water at 37°C. The buffer was adjusted to pH 7.4 with 1 M HCl.
2. 3.0 mL of 100 mM α-ketoglutarate solution, prepared by dissolving solid α-ketoglutarate monosodium salt in 100 mM Tris buffer.
3. 6.0 mL L-alanine solutions of varied concentration (see Table 2.1 below), prepared by dissolving solid L-alanine in 100 mM Tris buffer

The reaction cocktail was adjusted to pH 7.4 at 37°C with 1 M sodium hydroxide solution. A 2.90 mL volume of reaction cocktail was transferred to a 1 cm cuvette, which was placed in a heating block connected to a 37°C water bath, thereby ensuring the reaction occurred at physiological temperatures. Temperatures were constantly monitored with a thermometer. See Figure 2.3 for a schematic depiction of the ALAT reaction setup.

The reaction began upon the addition of 100 µL ALAT enzyme solution to the reaction cocktail, bringing the total reaction volume to 3.0 mL. ALAT solutions were prepared at various

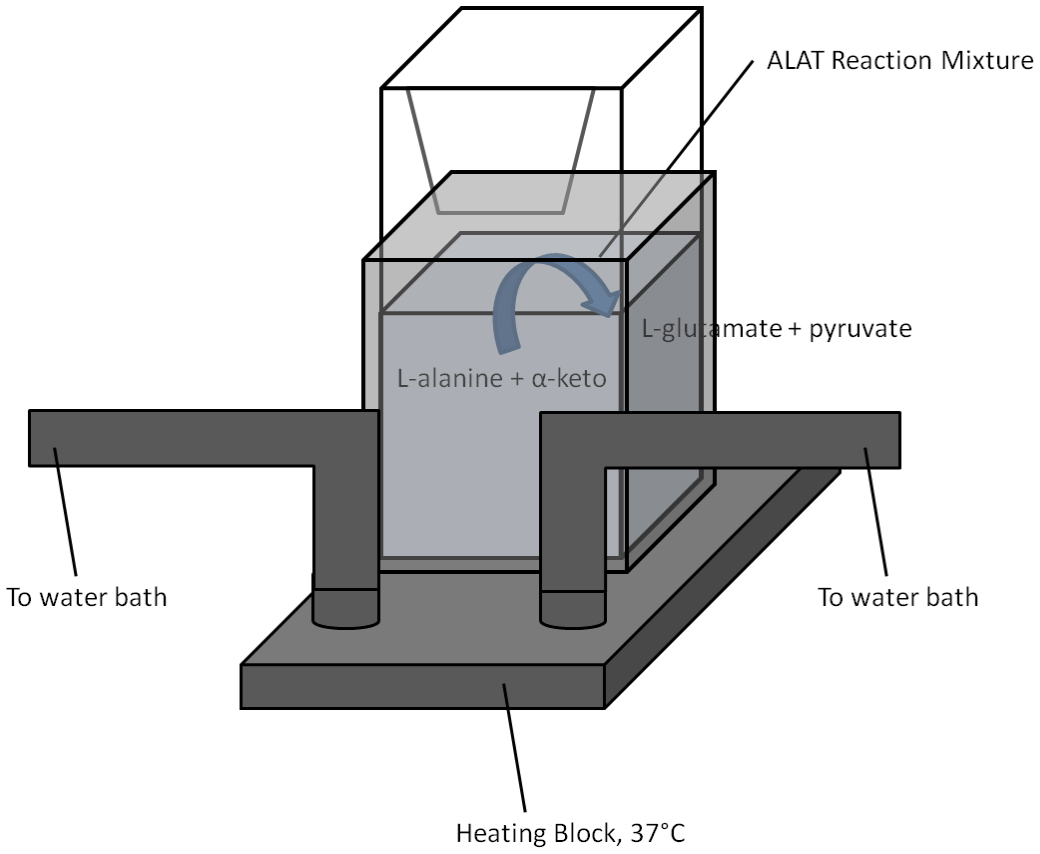

Figure 2.3. Alanine aminotransferase reaction setup. Two pipes connect the heating block to an external water reservoir heated to 37°C. The cuvette containing the reaction mixture is placed on top of the heating block for temperature control.

concentrations by dissolving lyophilized enzyme powder (mammalian ALAT from porcine heart tissue) in an appropriate volume of cold deionized water. The final concentrations of Tris and α-ketoglutarate in the reaction mixture were 93 mM Tris and 10 mM α-ketoglutarate. Each assay performed featured a different concentration of ALAT solution or a different concentration of L-alanine in the reaction cocktail. The assay concentrations of each are summarized in Table 2.1 below.

Table 2.1. L-alanine and ALAT concentrations in ALAT Reactions. The high L-alanine concentrations in assays #1-5 were intended to drive the reaction to the product side. A final working enzyme concentration of 150 U/mL ALAT was decided on based on the results of assays 1 though 5.

Assay #	Conc. L-alanine in reaction mixture (mM)	Conc. ALAT (U/mL)
1	200	0.1
2	200	0.2
3	200	1
4	200	150
5	200	600
6	20	150
7	2	150
8	0.2	150
9	0.8	150
10	0.4	150

Initial assays involved very high concentrations of either L-alanine or ALAT (orders of magnitude higher than physiological or protocol-based concentrations), in an effort to drive the reaction to the product side (i.e. the production of pyruvate and glutamate) as a proof of concept. Thus, the initial L-alanine concentrations were well above the established K_m value of 2.0 mM [18]. In later assays, concentrations of both L-alanine and ALAT were gradually altered in order to properly characterize the reaction. The ultimate goal was to ascertain a sufficient concentration of ALAT in order to obtain a reaction "completion time" of roughly 15-20 minutes while also

reducing L-alanine concentrations to near-physiological levels. Time to completion was taken as the time required for the current corresponding to the concentration of measured L-glutamate (see section 2.2.3 below) to reach a steady-state, indicating reaction equilibrium. "Blank" assays containing no ALAT enzyme were also performed with each experimental assay as a control, with all other experimental parameters being identical.

2.2.3. Glutamate Oxidase and Hydrogen Peroxide Reactions

The glutamate oxidase and hydrogen peroxide reactions were conducted in the YSI 1500 analyzer following proper calibration (see section 2.2.1 above). After the ALAT reaction was initiated by the addition of ALAT to the cuvette (see section 2.2.2), discrete 25 µL samples were periodically (approximately every 2-4 minutes) drawn from the cuvette using the capillary syringe-pette. The samples were then delivered to the 500 µL YSI analyzer chamber, after which the sensor was allowed to equilibrate for one minute as reactions (6) and (7) proceeded. The resulting current measurements were then recorded along with the elapsed assay times at which the individual samples were drawn from the ALAT reaction cuvette. Each complete assay consisting of the ALAT, GluOD and hydrogen peroxide reactions were allowed to run until the current measurements became relatively stable, unless they were terminated beforehand for reasons of inactivity (see section 2.3). The "completion time" varied depending on the L-alanine and ALAT concentrations of the reactions.

2.3 Results and Conclusions

Linear fit equations derived from YSI glutamate sensor calibrations were tested for accuracy with via back-calculations with standard current measurements (x = 0, 5, and 10 mM). All calculated concentrations were accurate to the nearest 1.0 mM. Figure 2.4 is an example of a

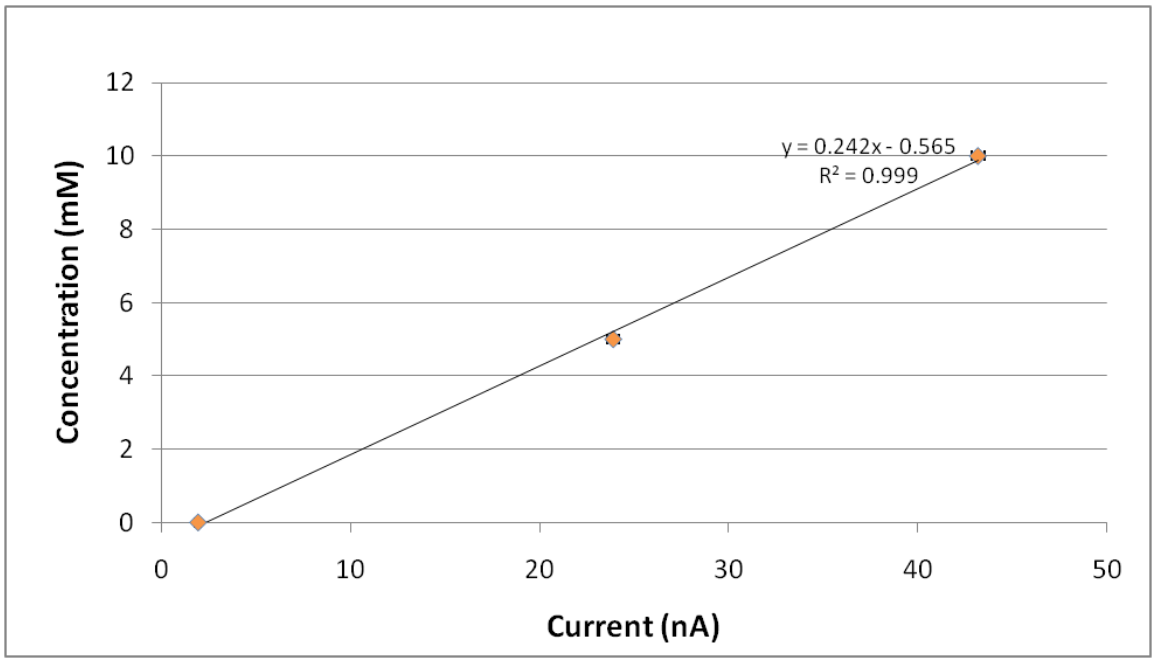

Figure 2.4. A representative glutamate calibration curve. Although the current is the dependent variable during calibration with known glutamate concentrations, it is presented as the independent variable so that the equation for the calibration line can be applied to measure currents of unknown samples. The number of samples was n = 6 for 0 mM and n = 3 for 5 and 10 mM. The horizontal error bars represent ±1 standard deviation.

typical representative curve that was obtained from the calibration procedure. Note that although the calibrations were performed by measuring the electrode response to known glutamate standard concentrations, the amperage is presented as the independent variable in the calibration curves so that the equation for the line of best fit could be directly used to calculate the concentrations of unknown samples when the amperages were measured.

Each individual assay ran for a different period of time to reach "completion", determined as the point at which the changes in concentration with each subsequent measurement became diminished, indicating the slowing of the reaction rate. Assays were also ceased if the YSI current measurements did not show any indication of reaching equilibrium after a particular period of time (around 10-12 minutes for most assays). This implied that the conditions of the assay, particularly the concentration of ALAT, are unacceptable for practical applications that would require timely measurements. Blank assays were somewhat arbitrary in length but were typically shorter than experimental assays, as non-reactivity was readily determined by only a few measurements. Table 2.2 summarizes the assay times for both the experimental and blank measurements.

Table 2.2. Assay times. Note that some assays ran for longer periods of time than others. This was either because 1) the reaction failed to slow (i.e. glutamate concentration did not reach a relatively stable value) after a certain period of time and were selectively ended or 2) because the reaction was arbitrarily extended in order to observe long-term behavior. The latter scenario was more likely when the reaction appeared to be reaching equilibrium, as in assays #4-10.

Assay #	Experimental Assay Time (sec)	Blank Assay Time (sec)
1	980	670
2	655	555
3	2102	1482
4	1786	1140
5	930	912
6	1005	680
7	1155	800
8	1250	800
9	1554	984
10	1569	984

The graphical results from each assay 1 through 10 can be found in the Appendix. The calibration curve and results from the experimental and blank assays are provided in each instance. In the latter two graphs, current measurements that are directly proportional to the glutamate concentrations are plotted against elapsed assay time, providing temporal measurement of the enzyme activity and reaction progress. Table 2.3 summarizes the results of each assay, including the initial and final amperage readings, the final calculated L-glutamate concentrations, and the sensitivities of the YSI electrode calculated from glutamate standard calibrations.

Table 2.3. Summary of L-alanine assays results via the detection of hydrogen peroxide.

Assay #	**Initial Amperage at t = 0 (nA)**	**Final Amperage at End of Assay (nA)**	**Final Calculated Glutamate Concentration (mM)**	**Approximate Electrode Sensitivity (mM/nA)**
1	2.06	3.55	0.28	0.24
2	2.03	4.62	0.54	0.23
3	1.95	31.13	6.97	0.24
4	2.08	41.54	9.22	0.23
5	2.11	2.15	9.81	0.27
6	1.92	23.44	6.1	0.29
7	2.23	6.75	1.34	0.30
8	2.08	2.72	0.08	0.30
9	4.29	6.02	0.68	0.37
10	3.44	4.49	0.27	0.36

In the first three assays (#1-3), the reactions did not appear to be slowing after 10-35 minutes, which implied that there was insufficient enzyme present in the reaction cocktail relative to the amount of L-alanine. Therefore, more substantial increases in enzyme concentration were needed. Following two additional assays at significantly higher enzyme concentrations (see Table 2.1), it was decided that 150 U/mL was appropriate, representing a compromise between achieving fast reaction rates and minimizing the consumption of enzyme. Thereafter, in an attempt to test this enzyme concentration under more physiologically relevant conditions, L-alanine concentrations used in the reaction cocktails of subsequent assays were gradually reduced from 200 mM to 20, 2, and 0.2-0.8 mM, the latter range representing normal physiological L-alanine concentrations in human blood [11, 19].

Overall, this experimental approach confirms the feasibility of an ALAT-based assay for the detection of L-alanine. The general procedure is simple to prepare and execute, and each sample injected into the YSI device produced a stable current measurement within one minute. Each experimental assay displayed increasing amperage with subsequent additions of reaction (6) samples from the corresponding cuvette. The degree to which the reaction reached "completion" (steady current measurements), however, depended upon the concentration of ALAT and, to a lesser extent, that of L-alanine. The time to completion was observed to be lower at higher concentrations of ALAT and lower concentrations of alanine, with a much more substantial dependence on ALAT. Although catalysis was certainly evident in reactions with very low concentrations of ALAT (see Appendix), these assays did not reach completion nor show signs of a reduction in catalytic rate after a reasonable period of time.

There are limitations that have been realized with the preliminary results obtained in these experiments. First, although the YSI analyzer displays current measurements with precision to the hundredth of a nanoampere, the device should generally only be considered marginally accurate to the nearest tenth of a nanoampere, as the hundredths denominations can be adversely affected by inherent electronic noise. In fact, extreme prudence would suggest that the measurements of the analyzer should only be trusted the nearest whole nanoampere. It is shown in the assay calibration curves that the range of sensitivities for the analyzer is approximately 0.23 - 0.37 millimolar per nanoampere. If the amperage can be measured to the nearest tenth of a nanoampere, then the sensitivity reaches an acceptable range of 0.02 - 0.04 millimolar per tenth of a nanoampere. However, if the conservative approach is taken and the current is read to the nearest whole nanoampere, the analyzer can only resolve glutamate concentrations to roughly the nearest one-quarter to one-third millimolar. Because the range of L-alanine in human serum is only approximately 0.3 - 0.9 mM [11, 19, 20], greater sensitivity would be ideal for physiological measurements. In addition, as previously stated, back-calculations for the glutamate calibration

curves were only accurate to the nearest whole millimolar, which would not be acceptable for measuring alanine concentrations within physiological ranges.

The second major limitation to the current procedure is that the alanine aminotransferase reaction does not convert all of the alanine present in the test sample into glutamate. As seen in Table 2.3, the "final" concentrations of glutamate detected in the samples, corresponding to the purported concentrations of alanine in the original samples, fall short of the actual alanine concentrations given in Table 2.1. This is entirely expected, as the equilibrium concentrations of all reactants and products are ultimately determined by the chemistry of the reaction. Additionally, in several cases the reaction was limited by the concentration of α-ketoglutarate (assays 1 through 6), and the maximum detected glutamate concentrations reflect this limitation. Therefore, while the YSI device was likely able to detect the actual glutamate concentration in the samples with acceptable accuracy, properly relating this to an "original" L-alanine concentration would also require alanine calibration reactions with at least two additional cocktails containing known concentrations of alanine that span the concentration range that the unknown sample would expect to fall within. Both calibration reactions would have to be run to "completion." As a note of caution, the behavior of the enzyme is expected to vary with different concentrations of alanine. Preliminary results indicate that within physiological ranges, the relationship between the "final" glutamate concentration and initial alanine concentration in the reaction cocktail is relatively linear at 150 U/mL ALAT (see Figure 2.5). However, this relationship becomes

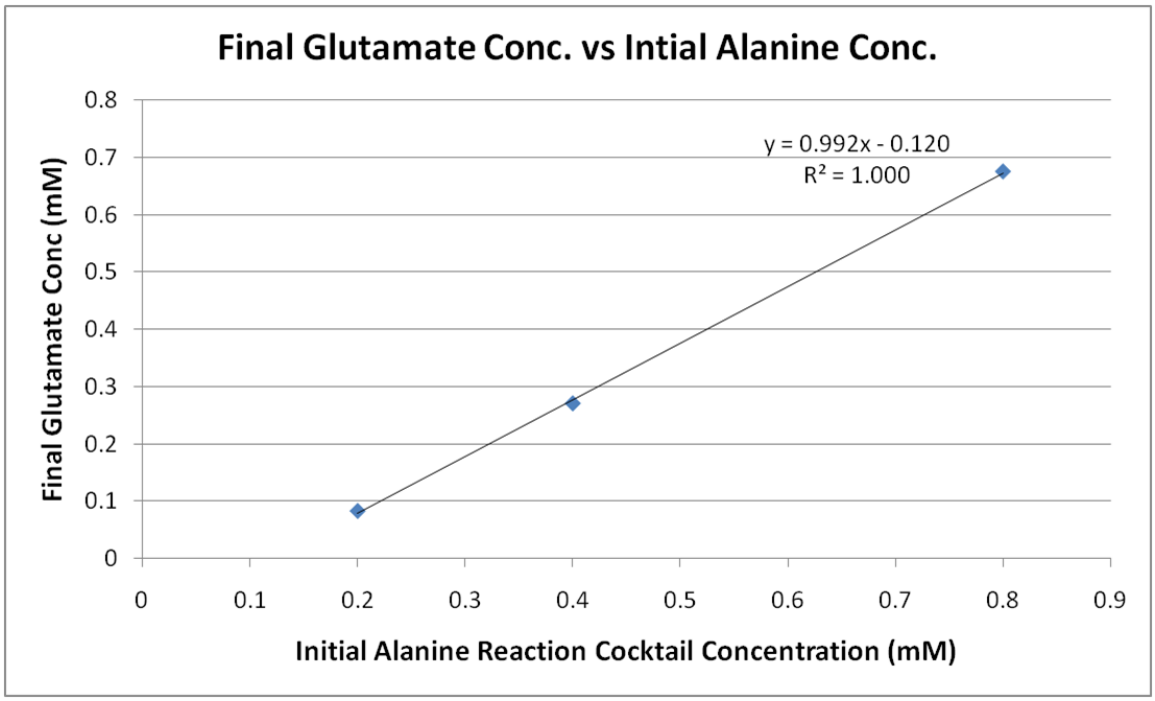

Figure 2.5. Hypothetical calibration curve for alanine reactions. The final glutamate concentrations calculated from the final current measurements are plotted as a function of the initial concentrations of L-alanine in the reaction mixture. This curve, constructed from actual data from the experiments herein, demonstrates a linear relationship between initial alanine concentration and final glutamate concentration at the end of the assay. The resulting currents would also be linear, and would allow the investigator to obtain an amperage calibration equation for alanine concentrations within this range.

nonlinear at higher concentrations of alanine. Consequently, the calibration curve may be defined by different classifications of lines of best fit, depending on concentration range of interest. The determination of this fitting with calibration reactions is tasked to the investigator.

Based on these preliminary results, it appears that the utilization a two-enzyme system consisting of ALAT and GluOD reactions is a sound concept. Unfortunately, the present exercise has been greatly limited by lack of sensitivity in the YSI device. Therefore, it was decided that an alternate strategy for L-alanine measurement should be explored in the form of oxygen detection.

Chapter III

Measurements via the Amperometric Detection of Oxygen

3.1. Introduction

The measurement of L-alanine via detection of hydrogen peroxide with an immobilized membrane biosensor was demonstrated as viable in chapter 2. However, the use of the YSI analyzer did not provide the sensitivity desired, specifically for measurements of alanine within physiological concentration ranges. In an attempt to achieve greater sensitivity, the process was attempted using a Hansatech oxygen detection system. The amperometric measurement of oxygen is a well-established method that has been employed in numerous biosensor applications, including the *in vivo* and *in vitro* detection of glucose and lactate [21], [22].

This oxygen measurement strategy is very similar in principle to the previous endeavor in that the alanine aminotransferase and glutamate oxidase reactions remain unchanged. Furthermore, the method of alanine measurement is also indirect, relying on the measurement of a metabolic species produced by the reactions. The primary difference is that where the YSI analyzer measures the hydrogen peroxide *produced* by reaction (7), the Hansatech system measures *oxygen* that is consumed by the reaction using an S1 type Clark electrode. While some electrochemical differences exist between hydrogen peroxide and oxygen detection[23], the primary motivation for attempting this scheme is the potential for large increases in sensitivity. The electrode control unit has a range of 0-2V, reporting potential to the nearest millivolt.

A general schematic illustration of a Clark-type electrode can be seen in Figure 3.1. The system is used to measure the concentration of oxygen of the sample in the reaction chamber,

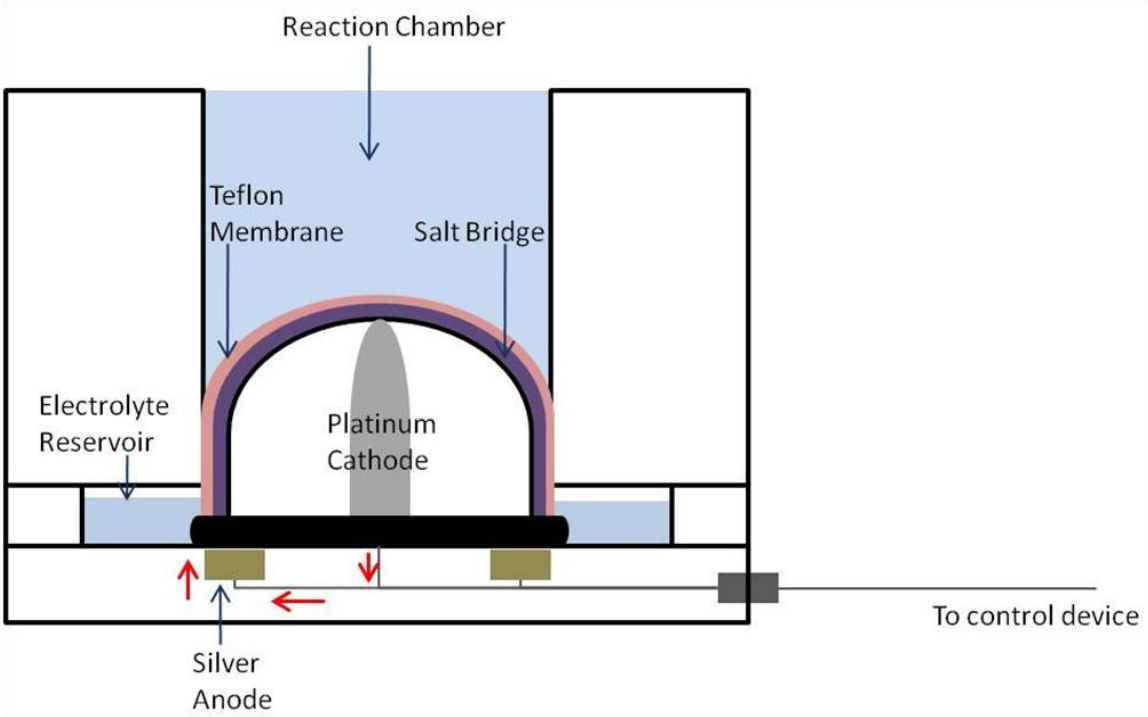

Figure 3.1. Schematic illustration of a Clark-type electrode. This diagram is specific to the electrode assembly used in the present experiments. The red arrows represent direction of current movement.

which is kept well-stirred so that an oxygen gradient does not form. An oxygen-permeable Teflon membrane is placed over the electrode assembly, separating it from the reaction chamber. This membrane also serves as a barrier to prevent the diffusion of reducible substrates to the sensor that would cause electroactive interference. A salt bridge is also placed below the Teflon membrane in order to complete the circuit and allow the movement of ions between the electrodes. A potentiostat maintains a constant potential between the two electrodes. Therefore, when oxygen permeates the membrane and diffuses to the cathode, it is electrochemically reduced, resulting in the movement of elections at a rate proportional to the rate of oxygen diffusion to the electrode. The rate at which oxygen can diffuse to the electrode is likewise proportional to the partial pressure (concentration) of oxygen in the solution. The consequent movement of elections due to oxygen reduction results in a measurable current, which is then reported by the Hansatech device as an equivalent voltage reading, given in millivolts. Thus, the amplitude of the signal is proportional to the oxygen concentration in the reaction chamber.

3.2. Setup of Experimental Equipment and Methods

3.2.1. Equipment Assembly

The oxygen detection sensor assembly consisted of three main components. A cylindrical reaction chamber hosted the Clark electrode and served as the site for the glutamate oxidation and oxygen detection reactions. The chamber featured a water jacket with connections to an external water bath for temperature regulation as well as an opening in the top of the chamber for the addition of buffer or substrate. The opening also served as an insertion point for the gas sparge needle (see section 3.2.2). The reaction cylinder was placed atop a stir platform, providing control over the rotational speed of the small magnetic stir bar within the chamber. Finally, the Clark electrode beneath within the reaction cylinder was connected to a control unit that reported the potential associated with the oxygen reduction reaction within the reaction chamber and allowed

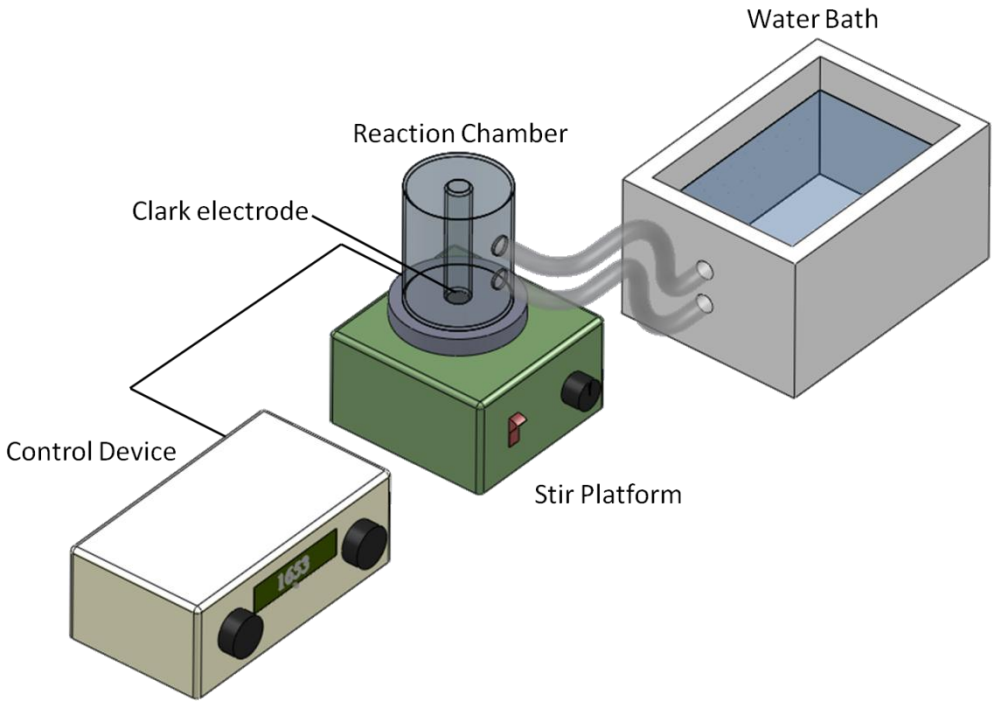

Figure 3.2. Experimental setup for the amperometric detection of oxygen. The Clark electrode sits beneath the reaction chamber in the cylinder. The control device has a 4-digit display and reports potential to the nearest millivolt.

the user to coarsely or finely adjust the gain of the device. The setup can be observed in Figure 3.2. When the sparging of gas into the reaction buffer was required, the sparge needle was connected to a benchtop gas valve with standard tubing and then inserted into the reaction chamber.

The membrane configuration on the Clark electrode required assembly for each test. Prior to inserting the electrode into the reaction cylinder and connecting it to the control unit, the electrode was carefully cleaned. Several drops of potassium chloride (KCl) electrolyte were added to the top of the platinum cathode and to the electrolyte reservoir. Next, a small piece of cigarette paper was placed over the cathode, covering the electrode dome, and dampened with additional KCl solution, thereby serving as a salt bridge connecting the cathode and anode. Lastly, a small rectangular section of Teflon was placed over the salt bridge layer, and the entire assembly was held into place with an elastomeric o-ring.

3.2.2. Clark Electrode Response with Gas Sparge

Prior to conducting reaction assays, the Clark electrode was first tested for responsiveness to changes in oxygen concentration within the chamber, the goal being to obtain a roughly linear relationship between the oxygen concentration in the reaction media and the voltage reported by the control unit. First, 1 mL YSI sensor buffer was added to the chamber. This buffer was assumed to have the same oxygen composition as the ambient air, approximately 21%. The voltage reported by the control unit at this concentration was noted. Next, gas containing 1% oxygen and 99% nitrogen was sparged into the buffer in the reaction chamber. The voltage on the control unit was monitored as the 1% oxygen sparge steadily decreased the concentration of oxygen in the buffer. Steady-state voltage at 1% oxygen was typically achieved in under 3 minutes, and was subsequently recorded. Finally, gas containing 10% oxygen and 90% nitrogen was sparged into the buffer, resulting in an increase in buffer oxygen concentration and a

corresponding increase in the voltage reported by the control unit. The voltage was again recorded once steady-state was achieved. The YSI buffer was replaced and the procedure repeated as necessary to obtain consistent voltage readings at each of the oxygen concentration. After a sufficient number of readings were obtained, the potentials were plotted against oxygen concentration to confirm that the response of the electrode was approximately linear.

3.2.3. L-Glutamate Standard Response Tests

The Hansatech oxygen sensor was tested for responsiveness and sensitivity to changing oxygen concentrations due to a glutamate oxidase reaction. Because glutamate and oxygen are consumed in equimolar amounts in the GluOD reaction, any observed drop in potential due to oxygen consumption could be quantitatively related to the amount of glutamate in the injected sample, which in turn is associated with the concentration of alanine in the original ALAT reaction. By again utilizing standard solutions to test the sensor's response, a plot of glutamate concentration vs. potential drop could be used to generate a line of best fit, thus allowing for the determination of the sensitivity of the sensor in mM of L-glutamate per millivolt of potential drop.

It was necessary to replicate as closely as possible the conditions of the GluOD reaction from chapter 2 to ensure that any difference in responsiveness or sensitivity was due to the sensor apparatus alone, thus allowing for a direct comparison between the two detection methods. Following reaction cylinder assembly and gas sparge calibration, the reaction chamber was drained and a YSI GluOD membrane was added to the reaction chamber and positioned directly on top of the Clark electrode. The stir bar was then placed on top of the GluOD membrane, very loosely holding the membrane down onto the electrode. The chamber was then refilled with 500 µL of fresh YSI buffer and the electrode was allowed to equilibrate to a steady-state voltage reading.

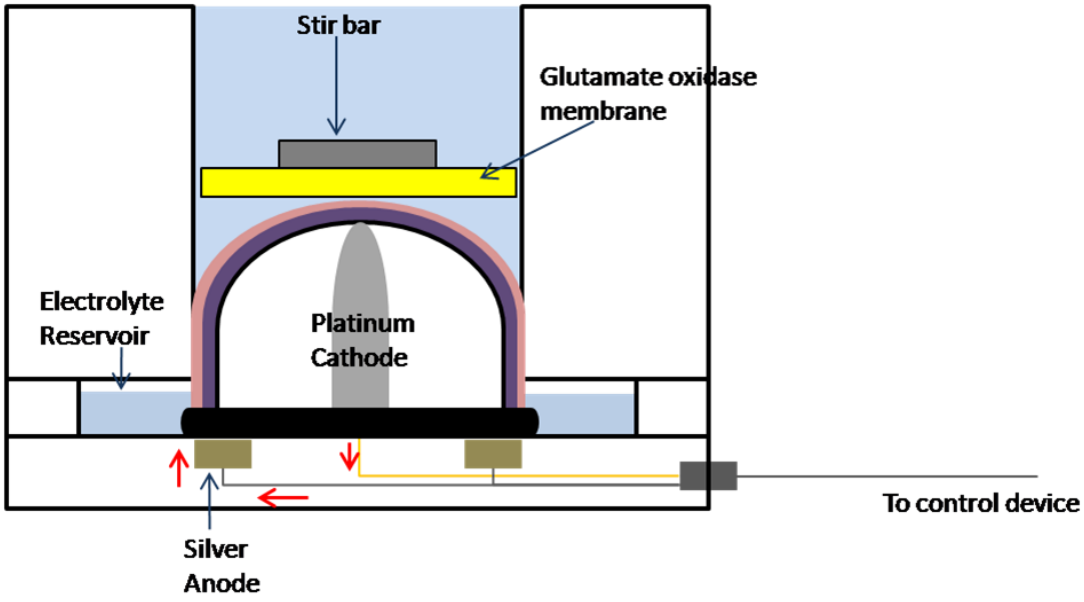

Figure 3.3. Clark electrode assembly with stir bar and immobilized glutamate oxidase membrane.

Figure 3.3 shows an updated assembly of the Clark electrode that includes the membrane and stir bar.

To test the sensor's response to glutamate, 5 mM and 10 mM L-glutamate standard solutions were pipetted to the reaction chamber in 25 µL volumes in a similar fashion as in section 2.2.1. The injection of an L-glutamate standard solution was expected to trigger a voltage drop, as the oxygen in the reaction chamber was consumed by the GluOD reaction. The injection would be followed by a period of stabilization where the sensor was allowed to reach a steady potential. However, it was quickly realized that this procedure did not result in consistent voltage drops following standard solution injections, and indeed several injections of standard did not produce any change in potential in preliminary testing (data not shown). Through rigorous experimentation, it was determined that because the membrane was only loosely placed on the electrode, oxygen was oftentimes able to diffuse around the membrane and reach the electrode largely unobstructed. Therefore, depending on the positioning of the membrane atop the Clark electrode, potential readings were sporadic as various amounts of oxygen diffused to the surface of the electrode to be reduced. As a result, it was not possible to verify that drops in voltage were in fact due to the consumption of oxygen by the GluOD reaction.

As a remedy to this issue, the membrane was more firmly secured to the top of the electrode in a crude manner using a pair of chemical spatulas. The spatulas were inserted into the reaction chamber and positioned along the edges of the membrane, providing additional weight to hold the membrane tightly against the electrode, as shown schematically in Figure 3.4. Upon the application of pressure on the membrane with the spatulas, a voltage drop was reported by the control unit, indicating that oxygen diffusion to the electrode was now limited by the membrane.

The steady-state potential achieved by the electrode following the "locking down" of the membrane served as a new baseline from which glutamate response tests could be performed. Multiple 25 µL volumes of 5 mM and 10 mM L-glutamate standard solutions were injected into

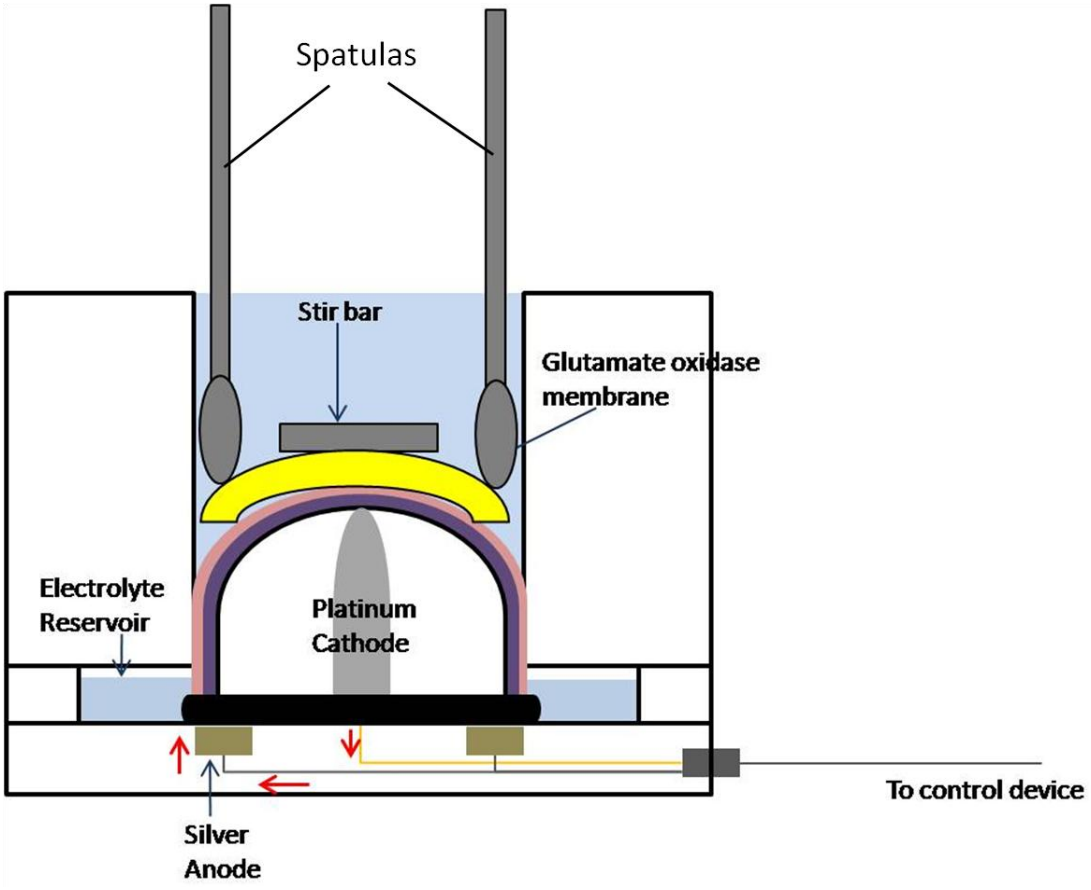

Figure 3.4. Chemical measurement spatulates were used to physically press the membrane down onto the electrode. This resulted in consistent voltage drops upon the addition of glutamate standards to the reaction chamber.

the chamber, resulting in GluOD catalysis, the consumption of oxygen, and consistent reductions in voltage reported by the control unit. Care was taken to avoid disturbing the spatulas, which would result in membrane becoming agitated and the voltage readings skewed. The final steady-state voltage was recorded following stabilization. The chamber was drained and thoroughly rinsed with YSI buffer following each standard injection. Final data analysis was performed on the net voltage drop from each injection instead of the final voltages. The net voltage drops were used to determine the sensitivity of the Clark electrode to GluOD-induced reductions in oxygen concentration.

3.3. Results and Conclusions

The Clark electrode's response to sparges of gas at different oxygen concentrations was rapid, typically reaching a new steady-state potential in less than one minute after the initiation of the sparge. A representative gas sparge response curve is shown in Figure 3.5, with the line of best fit indicating a loosely linear relationship between oxygen concentration and potential. Moreover, it was determined that the device offers a detection range of over 1200 mV for the sparged oxygen concentrations, though this entire range would not be utilized for subsequent glutamate tests (see below). Much like the YSI device, the exact steady-state values achieved with the different gas sparges (1%, 10%, and 21%) varied slightly with each sparge test, which can be attributed to minute differences in electrode assembly for each test (such as the amount of electrolyte in the reservoir, the size of the salt bride and Teflon membrane sections, etc) as well as natural deviation inherent of electronic equipment. Ultimately, the variation was insignificant and the general trend seen in Figure 3.5 was highly repeatable in multiple gas sparge tests.

With the addition of the glutamate oxidase membrane into the reaction chamber, the electrode's response to L-glutamate standard injections was tested. Beginning with fresh YSI solution, 25 µL glutamate injections at 5 mM and 10 mM resulted in measurable voltage drops

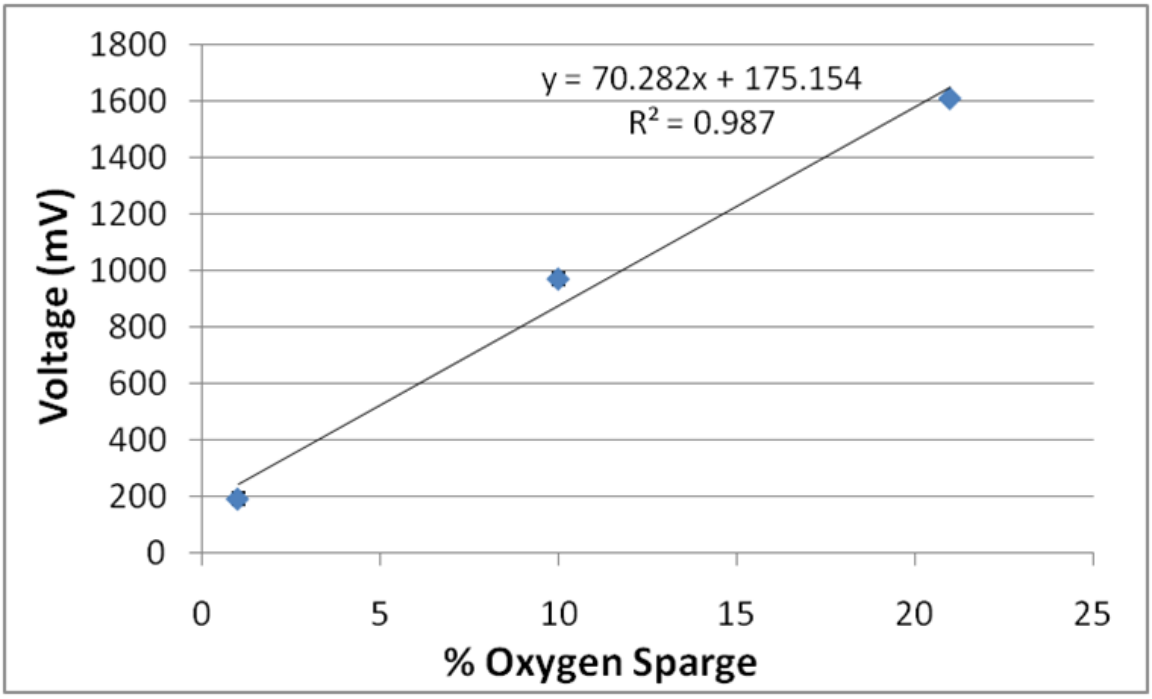

Figure 3.5. Gas sparge response curve. The response of the electrode was tested at 1%, 10%, and 21% oxygen, with n = 2 for each point. The vertical error bars represent ±1 standard deviation.

reported by the Hansatech control device. The time required to achieve a new steady-state following standard injection was typically less than three minutes. Similar to the gas sparge tests, there was considerable variation in the initial (0 mM), and final (5 mM and 10 mM) steady-state voltages observed during the glutamate injection tests. Table 3.1 lists the ranges and average values for the voltage drops, which was used as the criteria for quantifying the electrode response. Figure 3.6 presents this data in graphical form, with the average voltage drop plotted as a function of the concentration of the injected glutamate standard. There is a relatively strong linear relationship between the voltage drop and concentration of glutamate.

Table 3.1. Summary of voltage drop in response to the addition of 5 mM and 10 mM glutamate standard solutions.

	Range of Voltage Drop (mV)	Average Voltage Drop (mV)
Initial Voltage	N/A	0
5 mM Glutamate Addition	39 - 45	42
10 mM Glutamate Addition	67 - 76	72

To reiterate, the primary motivation for exploring the application of a Clark electrode in the detection of L-glutamate (and ultimately the detection of L-alanine) was to achieve a greater degree of sensitivity in the detection scheme. According to the calibration curve in Figure 3.6, a sensitivity of roughly 0.140 millimolar per millivolt was obtained using this oxygen sensing method. In comparison to the sensitivity values calculated from the YSI detection data, the Hansatech Clark electrode was shown to be approximately 1.6 to 2.5 times more sensitive than the hydrogen peroxide detection method utilized in Chapter 2 (assuming that the YSI measurements are only accurate to the nearest whole nanoampere). These results suggest that the present procedure for the amperometric detection of oxygen allows for greater sensitivity than does the detection of hydrogen peroxide, which in turns allow for more exact measurements of glutamate. However, it still does not provide enough sensitivity to detect glutamate

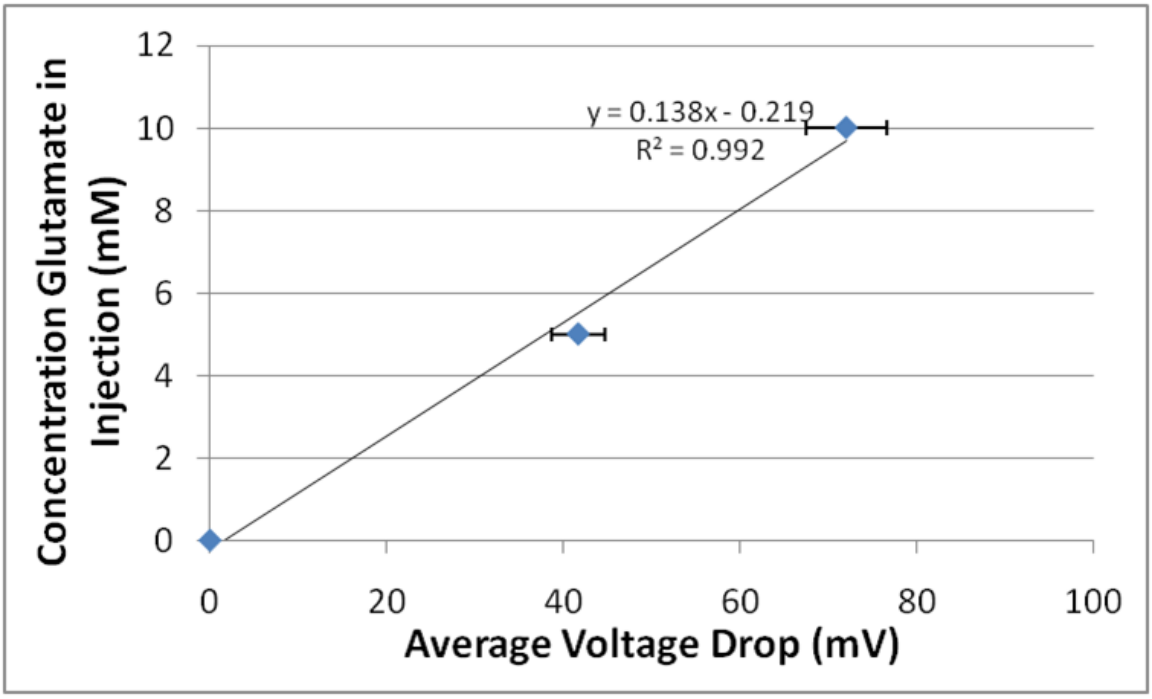

Figure 3.6. Graphical representation of electrode response to additions of 5 and 10 mM glutamate solutions. There is a linear relationship between the voltage drop and glutamate concentration. The number of samples was n = 3 for each group. The horizontal error bars represent ±1 standard deviation.

concentrations to the nearest tenth of a millimolar, which would be ideal and perhaps even necessary for physiological measurements. Additionally, the Clark electrode is also subject to electronic noise, which may further limit the accuracy of the device at the millivolt scale.

The most probable cause for the apparent lack of sensitivity was the utilization of the YSI glutamate oxidase membrane in the Hansatech device, thereby combining two components that were not designed to work with one-another. Section 3.2.3 discussed the crude restraint procedure used to minimize the motion of the membrane, allowing for the detection of changes in oxygen concentration with the addition of glutamate standard. It is possible that more robust and reliable membrane security methods may contribute to greater sensitivity by further regulating the amount of oxygen diffusing freely to the electrode. For example, incorporating the GluOD membrane into the initial electrode assembly, where it may be kept secured by the o-ring along with the salt bridge and Teflon layers, may improve the response range of the electrode.

Additionally, it is also possible that sensitivity was directly limited by the membrane construction itself. As the membrane was specifically designed for the detection of hydrogen peroxide, the composition of its layers, and particularly the inclusion of the cellulose acetate layer, may not been conducive to the diffusion of oxygen, which limits its utility when used with a Clark electrode. Specifically, because the Clark electrode already includes a Teflon membrane, the inclusion of the cellulose acetate dialysis membrane may be redundant and obstructive. Therefore, a future endeavor would be the fabrication a custom GluOD membrane that addresses these concerns. While options abound for the selection of the appropriate membrane constituents, a popular method for creating immobilized enzyme membranes utilizes bovine serum albumin as the base material and glutaraldehyde as a crosslinker [14],[24]. Literature review and experimentation will likely be necessary to ascertain the appropriate concentrations of BSA, glutaraldehyde, and GluOD to use in the construction of a membrane for this application, as well as to explore the effects of enzyme loading, temperature, and pH on sensor functionality.

However, if these properties can be characterized and exploited, then the application of an oxygen electrode in L-alanine detection may very well be realized.

Chapter IV

Conclusions

4.1. Conclusions from Experimentation

The alanine aminotransferase reaction was tested as a plausible avenue for the *in vitro* conversion of L-alanine to L-glutamate in stoichiometrically equivalent amounts. The resulting L-glutamate was then subjected to an oxidation reaction catalyzed by L-glutamate oxidase, after which the concentration of glutamate (and therefore alanine) was measured by two separate amperometric means: the oxidation of hydrogen peroxide and the reduction of oxygen. Measurements made with hydrogen peroxide detection demonstrated high consistency and extremely fast response times, but lacked the desired amount sensitivity. The oxygen detection method possessed a greater detection range and sensitivity, but was marred by issues of membrane stabilization and insecure contact with the electrode. Nevertheless, these experiments have confirmed the feasibility of the use of ALAT as the primary enzyme in an L-alanine detection scheme. Moreover, the amperometric detection strategy explored in this investigation has notable advantages over traditional fluorometric and colorimetric methods in that it is faster, does not require any cofactors, and can be prepared easily with stock Tris buffer and α-ketoglutarate solutions, both of which can be prepared well in advance of the assay and stored in bulk.

4.2. Future Directions

The greatest limitation realized from these experiments was the sensitivity of both of the L-glutamate detection strategies. While options for enhancing the sensitivity in the hydrogen peroxide detection mechanism are limited due to the proprietary nature of the YSI device, there remain several potential opportunities for improving both the the performance of the oxygen electrode. Future experiments might explore the creation and characterization of a customized immobilized enzyme membrane to improve sensitivity. Additionally, it is also possible that the reaction time of the ALAT step can be reduced by moving the reaction into a well-agitated, temperature controlled environment, thereby decreasing total assay times.

An ultimate goal would be to incorporate this two-step reaction into a single integrated sensor that is altogether practical, convenient, and superior to the AlaDH- and PyOD-based sensors that have been developed by other investigators. Because the methodology describes a system that is not reagentless, an *in vivo* probe for continuous alanine detection will probably not be possible. On the other hand, a benchtop sensor is conceivably attainable. Numerous engineering and biochemical hurdles must be traversed before such a device is realized. However, it may eventually serve as an invaluable tool in clinics and research laboratories for the rapid detection of L-alanine.

REFERENCES

1. Felig, P., Pozefsky, T., Marliss, E., and G.F. Cahill, *Alanine: Key Role in Gluconeogenesis.* Science, 1970. **167**(3920): p. 1003-1004.

2. Widmaier, E.P., Raff, H., and K.T. Strang., *Vander Human Physiology: The Mechanisms of Body Function*. 2005, Boston: McGraw-Hill.

3. Lehninger, A., Nelson, D., and M. Cox, *Lehninger Principles of Biochemistry*. 2005, New York: W.H. Freeman.

4. Court, J.M., Dunlop, M.E., and T.J.C. Boulton, *Effect of ephedrine in ketotic hypoglycaemia.* Archives of Disease in Childhood, 1974. **49**(63).

5. Holmes, E., Nicholson, J.K., and P. Elliott, *Human metabolic phenotype diversity and its association with diet and blood pressure.* Nature Letters, 2008. **453**.

6. Weicker, H., Hagele, H., Kornes, B., and A. Werner, *Determination of Alanine, Lactate, Pyruvate, Beta-Hydroxybutyrate, and Acetoacetate by Flow INjection Analysis.* Int. J. Sports Med., 1984. **5**: p. 47-54.

7. Gilis, M., Durliat, H., and M. Comtat, *Amperometric biosensors for L-alanine and pyruvate assays in biological fluids.* Analytica Chimica Acta, 1997. **335**: p. 235-240.

8. Marchelli, R., Dossena, A., and G. Palla, *The potential of enantioselective analysis as a quality control tool.* Trends in Food Science & Technology, 1996. **7**.

9. Esteban, G., *Monitoring Viable Cell Density for Improved Bioreactor Control*, in *BioProcess International*. 2005.

10. Ohman, L.L., J., and L. Haggstrom, *Induction of a metabolic switch in insect cells by substrate-limited fed batch cultures.* Appl Microbiol Biotechnol, 1995. **43**: p. 1006-1013.

11. BioVision, *L-Alanine Assay Kit*. 2010.

12. Favre, E.P., P., and P. Peringer, *Automated HPLC Monitoring of Glucose, Glutamine, Lactate and Alanine on Suspended Mammalian Cell Reactors.* Biotechnology Techniques, 1990. **4**(5): p. 315-320.

13. Kwan, R., Hon P., and R. Rennenberg, *Amperometric biosensor for rapid determination of alanine*. Analytica Chimica Acta, 2004. **523**: p. 81-88.

14. D'Amico, L., Basilio, A., Luo, S. and J. Yeap, *The Design and Development of an Enzyme Immobilized Alanine Sensor*. 2009, University of California, San Diego: La Jolla.

15. Karl, I.E., Pagliara, A.S., and D.M. Kipnis, *A Microfluorometric Enzymatic Assay for the Determination of Alanine and Pyruvate in Plasma and Tissues.* J. Lab. Clin. Med., 1972. **80**: p. 434-441.

16. *YSI 2357 Buffer Concentrate Kit; MSDS No. A95009F*
2009, YSI, Inc: Yellow Springs, OH.

17. Sigma-Aldrich, *Enzymatic Assay of GLUTAMIC-PYRUVIC TRANSAMINASE*. 1993.

18. G. De Rosa, B., T.L., and RW Swick, *Isolation and characterization of mitochondrial alanine aminotransferase from porcine tissue.* Biochim Biophys Acta, 1979. **567**(1): p. 116-124.

19. McMenamy, R.H., Lund, C., and J.L. Oncley, *Unbound Amino Acid Concentrations in Human Blood Plasmas.* J Clin Invest, 1957. **36**(12): p. 1672-1679.

20. Gutman, G.E., and B. Alexander, *Studies of Amino Acid Metabolism I: Blood Glycin and Alanine and their Relationship to the Total Amino Acids in Normal Subjects.* J. Biol. Chem, 1947. **168**: p. 527-536.

21. Armour, J.C., *Implantation of Glucose Sensors*, in *Engineering Sciences (Bioengineering)*. 1988, University of California, San Diego: La Jolla.

22. Baker, D.A., and D.A. Gough, *A Continuous, Implantable Lactate Sensor.* Anal. Chem, 1995. **67**(9): p. 1536-1540.

23. Gough, D., *The Latest on Long Term Implantable Glucose Sensors*. 2011: La Jolla.

24. Basu, A., Chattopadhyay, P, Roychudhuri, U, and R. Chakraborty, *Development of biosensor based on immobilized L-glutamate oxidase for determination of monosodium glutamate in food.* Indian J. Exp. Bio, 2006. **44**: p. 392-398.

APPENDIX

The following graphs summarize the results from the alanine assays in Chapter 2. The graphs for Elapsed Time vs. Amperage are shown for both the experimental and blank assays, as well as the calibration curves for each assay. In the calibration curves, the error bars represent ±1 standard deviation.

Assay #1

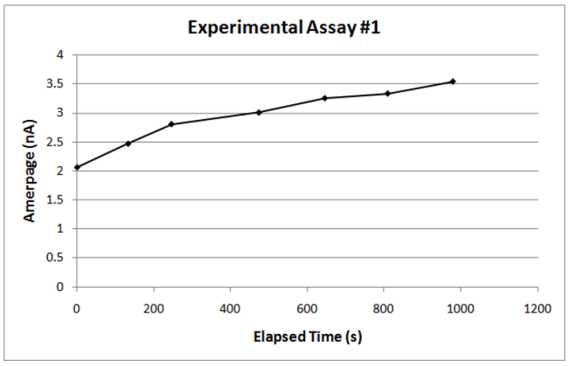

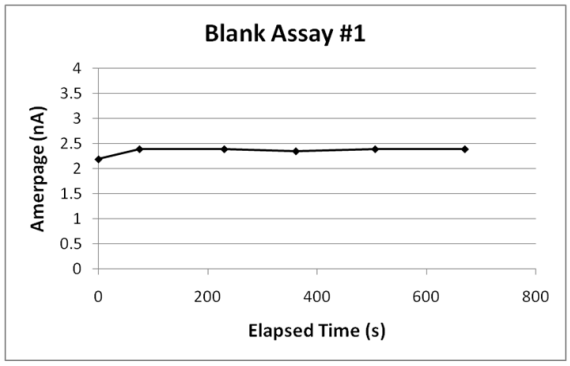

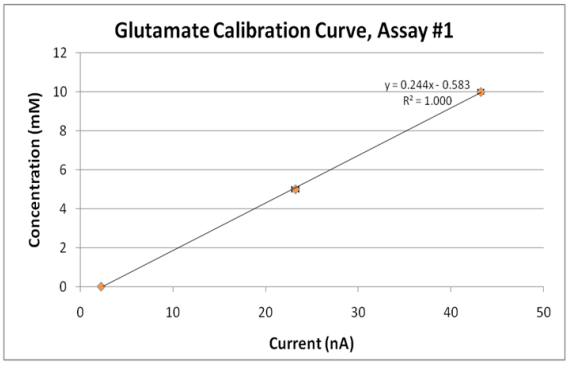

Assay #2

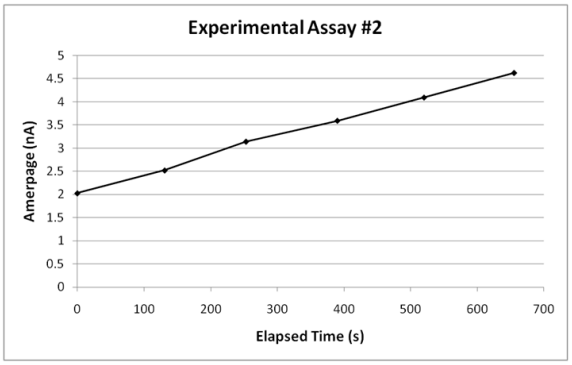
Experimental Assay #2
Amerpage (nA)
Elapsed Time (s)
0
0.5
1
1.5
2
2.5
3
3.5
4
4.5
5
0
100
200
300
400
500
600
700

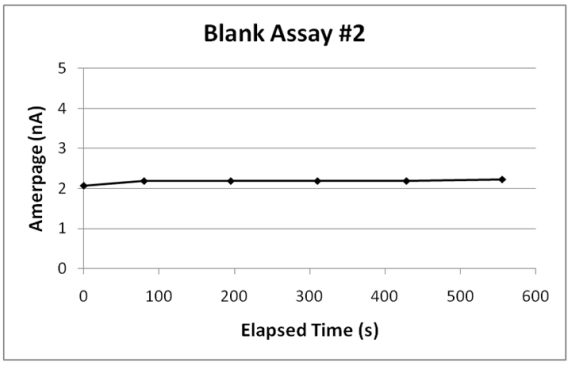
Blank Assay #2
Amerpage (nA)
Elapsed Time (s)
0
1
2
3
4
5
0
100
200
300
400
500
600

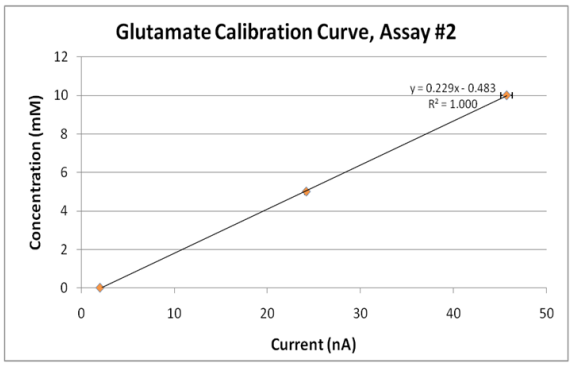
Glutamate Calibration Curve, Assay #2
Concentration (mM)
Current (nA)
y = 0.229x - 0.483
R² = 1.000
0
2
4
6
8
10
12
0
10
20
30
40
50

Assay #3

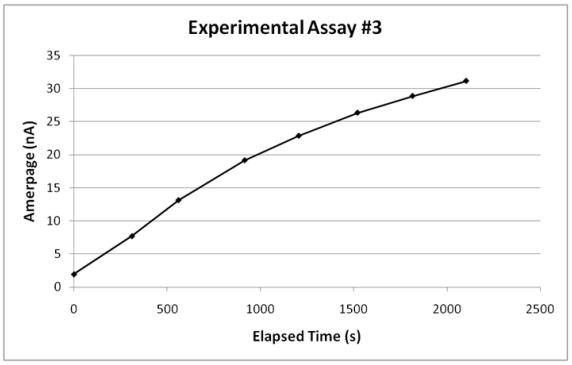
Experimental Assay #3
Amerpage (nA)
Elapsed Time (s)
0
5
10
15
20
25
30
35
0
500
1000
1500
2000
2500

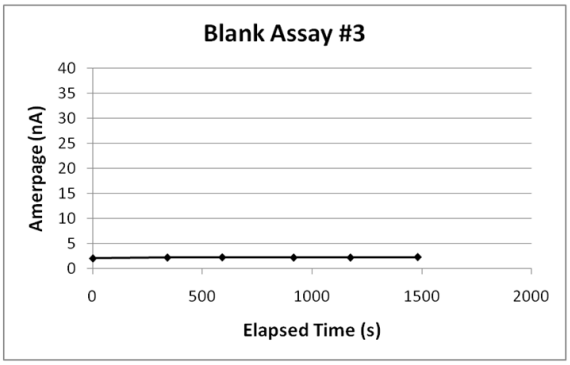
Blank Assay #3
Amerpage (nA)
Elapsed Time (s)
0
5
10
15
20
25
30
35
40
0
500
1000
1500
2000

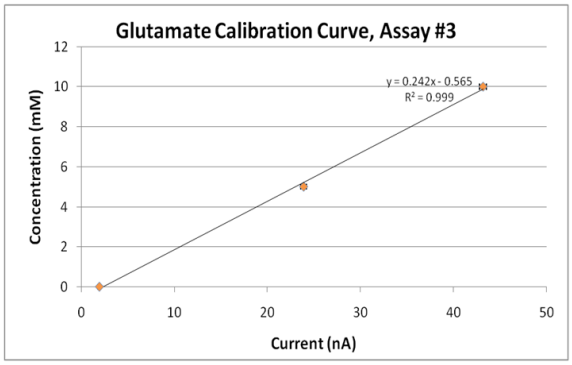
Glutamate Calibration Curve, Assay #3
y = 0.242x - 0.565
R² = 0.999
Concentration (mM)
Current (nA)
0
2
4
6
8
10
12
0
10
20
30
40
50

Assay #4

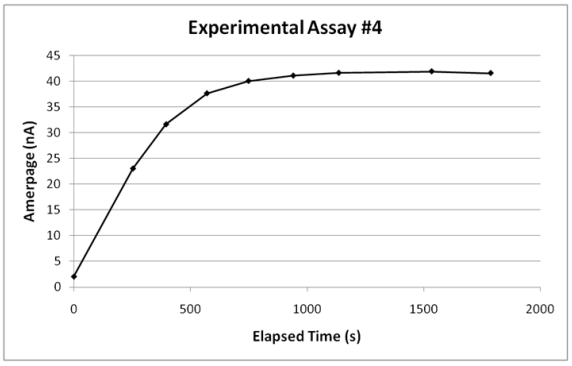
Experimental Assay #4
Amerpage (nA)
Elapsed Time (s)
0
5
10
15
20
25
30
35
40
45
0
500
1000
1500
2000

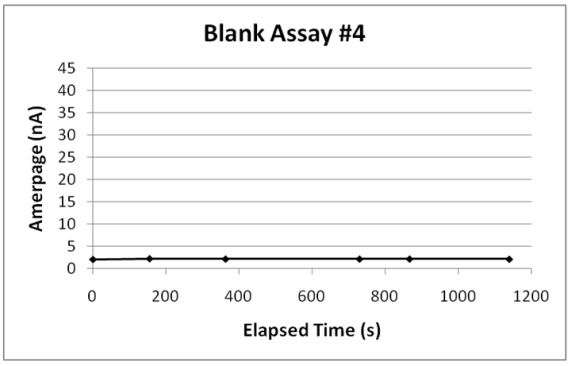
Blank Assay #4
Amerpage (nA)
Elapsed Time (s)
0
5
10
15
20
25
30
35
40
45
0
200
400
600
800
1000
1200

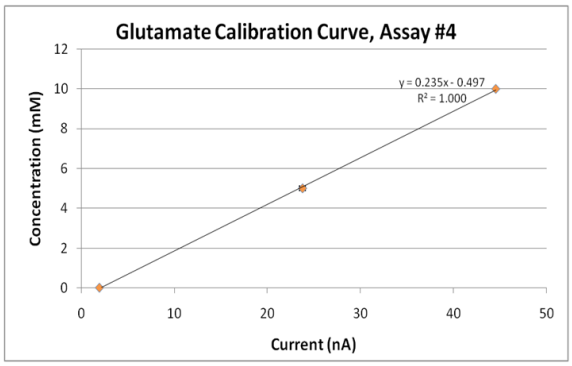
Glutamate Calibration Curve, Assay #4
y = 0.235x - 0.497
R² = 1.000
Concentration (mM)
Current (nA)
0
2
4
6
8
10
12
0
10
20
30
40
50

Assay #5

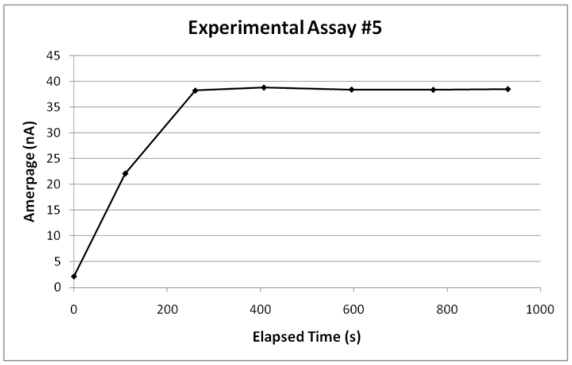
Experimental Assay #5
Amerpage (nA)
Elapsed Time (s)
0
5
10
15
20
25
30
35
40
45
0
200
400
600
800
1000

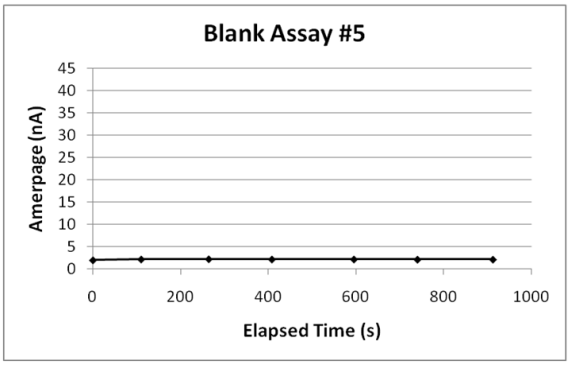
Blank Assay #5
Amerpage (nA)
Elapsed Time (s)
0
5
10
15
20
25
30
35
40
45
0
200
400
600
800
1000

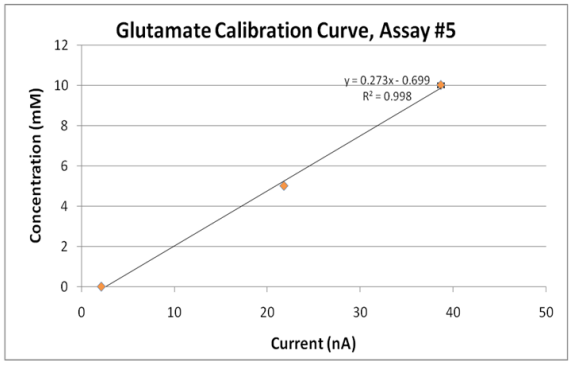
Glutamate Calibration Curve, Assay #5
y = 0.273x - 0.699
R² = 0.998
Concentration (mM)
Current (nA)
0
2
4
6
8
10
12
0
10
20
30
40
50

Assay #6

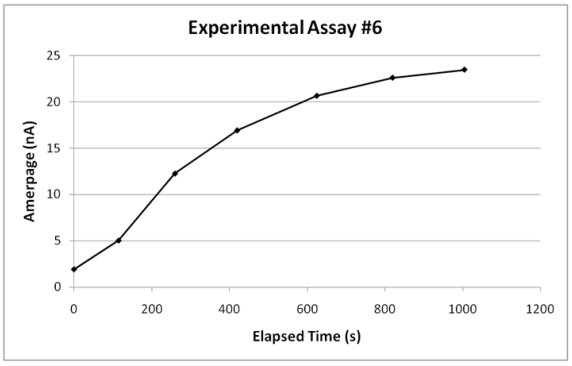
Experimental Assay #6
Amerpage (nA)
Elapsed Time (s)
0
5
10
15
20
25
0
200
400
600
800
1000
1200

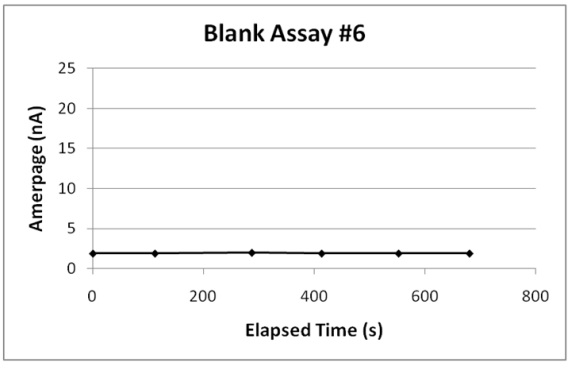
Blank Assay #6
Amerpage (nA)
Elapsed Time (s)
0
5
10
15
20
25
0
200
400
600
800

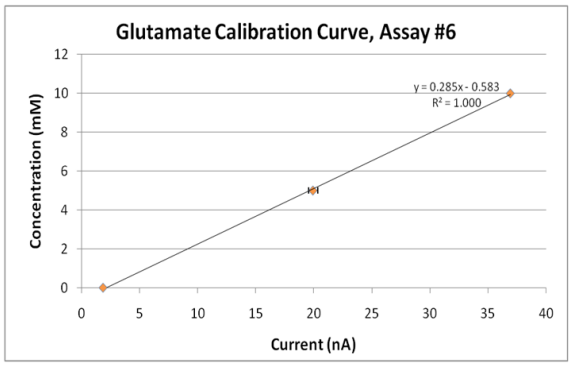
Glutamate Calibration Curve, Assay #6
Concentration (mM)
Current (nA)
y = 0.285x - 0.583
R² = 1.000
0
2
4
6
8
10
12
0
5
10
15
20
25
30
35
40

Assay #7

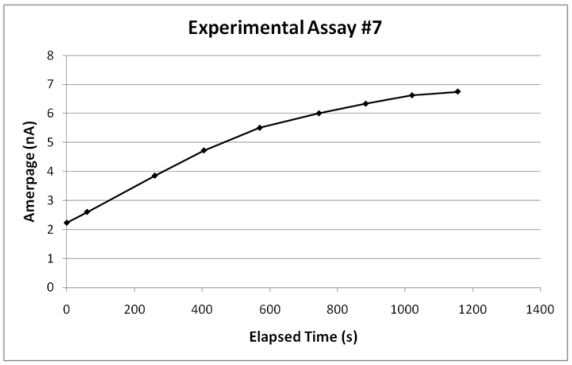
Experimental Assay #7
Amerpage (nA)
Elapsed Time (s)
0
1
2
3
4
5
6
7
8
0
200
400
600
800
1000
1200
1400

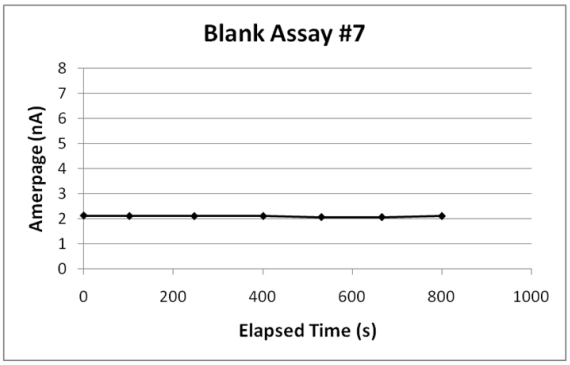
Blank Assay #7
Amerpage (nA)
Elapsed Time (s)
0
1
2
3
4
5
6
7
8
0
200
400
600
800
1000

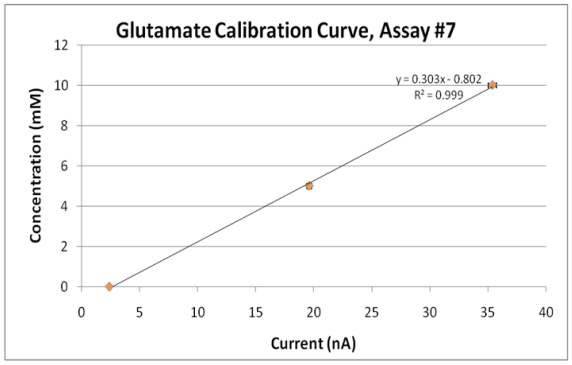
Glutamate Calibration Curve, Assay #7
y = 0.303x - 0.802
R² = 0.999
Concentration (mM)
Current (nA)
0
2
4
6
8
10
12
0
5
10
15
20
25
30
35
40

Assay #8

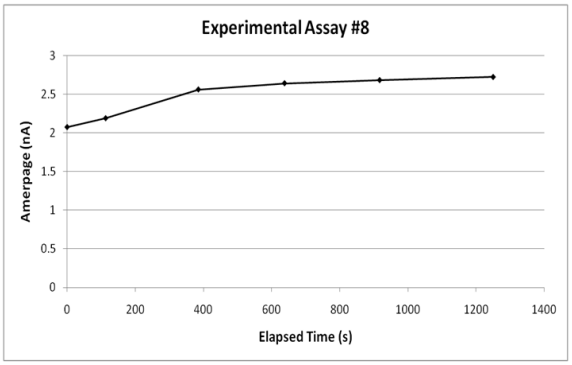
Experimental Assay #8
Amerpage (nA)
Elapsed Time (s)
0
0.5
1
1.5
2
2.5
3
0
200
400
600
800
1000
1200
1400

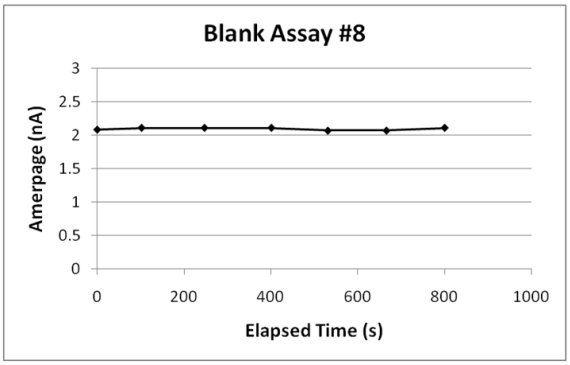
Blank Assay #8
Amerpage (nA)
Elapsed Time (s)
0
0.5
1
1.5
2
2.5
3
0
200
400
600
800
1000

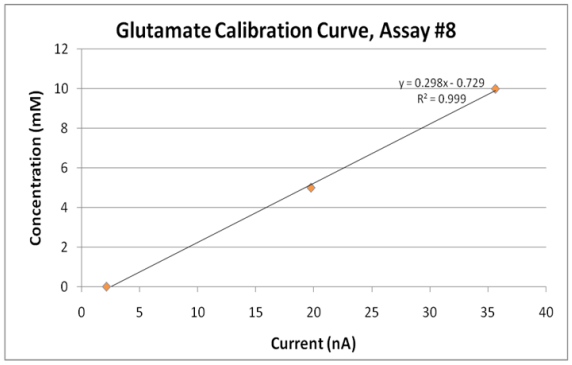
Glutamate Calibration Curve, Assay #8
y = 0.298x - 0.729
R² = 0.999
Concentration (mM)
Current (nA)
0
2
4
6
8
10
12
0
5
10
15
20
25
30
35
40

Assay #9

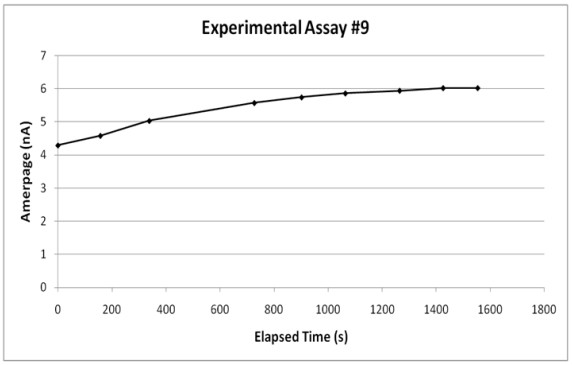
Experimental Assay #9
Amerpage (nA)
Elapsed Time (s)
0
1
2
3
4
5
6
7
0
200
400
600
800
1000
1200
1400
1600
1800

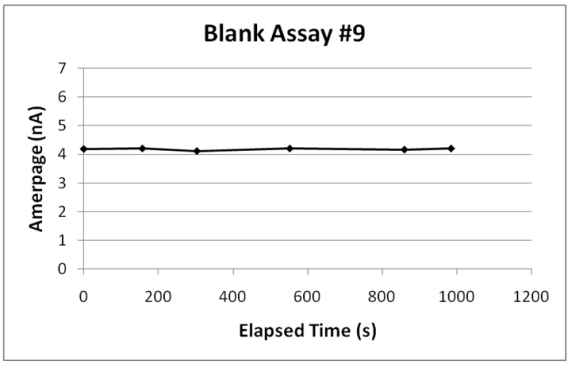
Blank Assay #9
Amerpage (nA)
Elapsed Time (s)
0
1
2
3
4
5
6
7
0
200
400
600
800
1000
1200

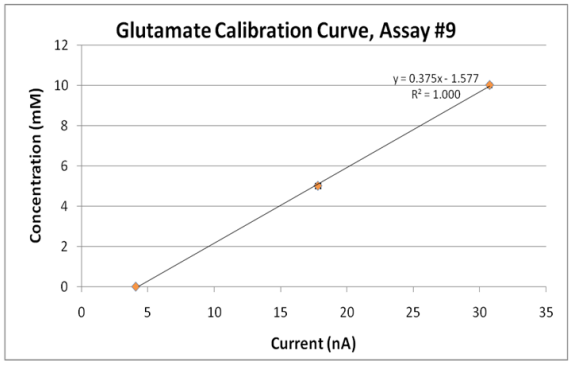
Glutamate Calibration Curve, Assay #9
y = 0.375x - 1.577
R² = 1.000
Concentration (mM)
Current (nA)
0
2
4
6
8
10
12
0
5
10
15
20
25
30
35

Assay #10

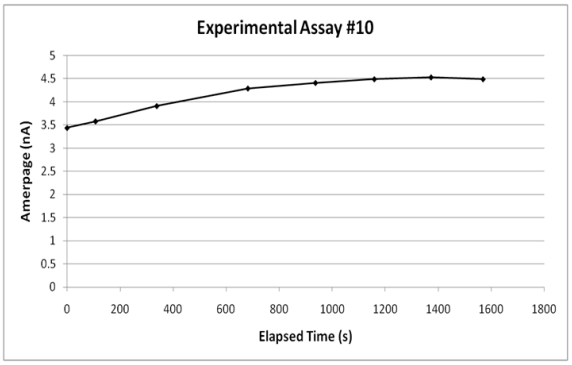
Experimental Assay #10
Amerpage (nA)
Elapsed Time (s)
0
0.5
1
1.5
2
2.5
3
3.5
4
4.5
5
0
200
400
600
800
1000
1200
1400
1600
1800

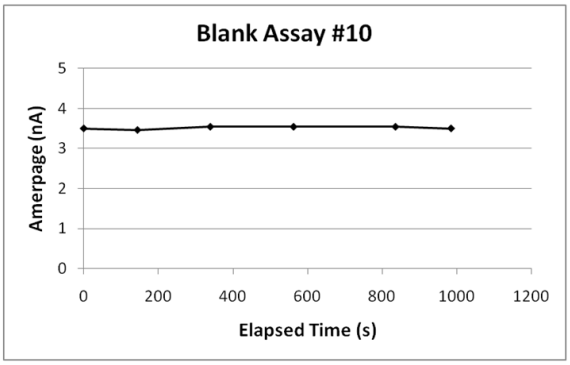
Blank Assay #10
Amerpage (nA)
Elapsed Time (s)
0
1
2
3
4
5
0
200
400
600
800
1000
1200

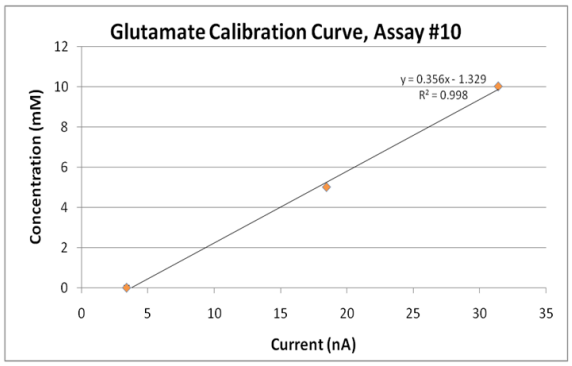
Glutamate Calibration Curve, Assay #10
y = 0.356x - 1.329
R² = 0.998
Concentration (mM)
Current (nA)
0
2
4
6
8
10
12
0
5
10
15
20
25
30
35